recent trials than in the older trials (6.5 and 4.4 months, respectively, $P < 0.0001$). The average proportion of median OS accounted for by median PPS significantly increased from 45.9% in older trials to 54.9% in recent trials ($P < 0.0001$).

relation between OS and either PFS or PPS

The relation between median OS and either median PFS or median PPS for the 151 treatment arms of the 69 trials is shown in Figures 2 and 3, respectively. We found that median PPS was strongly associated with median OS ($r = 0.82$, $P < 0.0001$) on the basis of Spearman's correlation coefficient, whereas median PFS was more moderately correlated with median OS ($r = 0.43$, $P < 0.0001$). The association between median OS and median PPS in recent trials ($r = 0.89$, $P < 0.0001$) was stronger than that in older trials ($r = 0.66$, $P < 0.0001$), whereas the correlation between median OS and median PFS in recent trials ($r = 0.55$, $P < 0.0001$) was similar to that in older trials ($r = 0.44$, $P < 0.0001$).

Table 1. Characteristics of the 69 phase III trials for advanced non-small-cell lung cancer included in the present analysis

Trial characteristics	
Median no. of patients per trial (range)	433 (153–1725)
Percentage of male patients (median)[a]	70.2
Percentage of adenocarcinoma patients[b]	51.2
Average of median age (years)[c]	62.3
Primary end point (no. of trials)	
OS	53
PFS or TTP	10
Response rate	3
Quality of life or toxicity	3
End point based on tumor assessment	
TTP	39
PFS	30
No. of treatment arms	
2	58
3	9
4	2

[a]One trial was excluded (data were not shown).
[b]Five trials were excluded (data were not shown).
[c]One trial was excluded (data were not shown).
OS, overall survival; PFS, progression-free survival; TTP, time to progression.

discussion

In the present study, we defined median PPS as median OS minus median PFS for each treatment arm of phase III trials for chemotherapy-naive patients with advanced NSCLC, as previously described [10, 12]. We also investigated the relation between median OS and either median PPS or median PFS by correlation analysis and found that median OS was more strongly associated with median PPS than with median PFS. Moreover, we also found that the correlation between median PPS and median OS was more pronounced in recent trials than in older trials and that median PPS was longer in recent trials than in older trials. This recent prolongation of PPS is likely the result of the increasing number of active compounds, such as docetaxel, pemetrexed, and epidermal growth factor receptor–tyrosine kinase inhibitors (EGFR-TKIs), which are available for second- or third-line chemotherapy in advanced NSCLC. One trial from a decade ago, when pemetrexed and EGFR-TKIs were not available, reported that only ~20% of patients received second-line chemotherapy [13]. In contrast, in the AVAiL trial, a recent large phase III trial that investigated the efficacy of cisplatin–gemcitabine with or without bevacizumab, second-line chemotherapy was administered in >60% of patients [8, 9]. Clinical trials of chemotherapy for patients with refractory NSCLC yielded a median OS of 5–8 months [14–17], which is similar to the median PPS for recent trials in our analysis. The recent widespread use of active second- and third-line therapies thus appears to have contributed to a prolongation of PPS in patients with advanced NSCLC.

Broglio and Berry [12] recently focused on PPS, which they termed survival postprogression (SPP) and defined as OS minus PFS, in a hypothetical clinical trial setting under the assumption that there was a treatment difference in PFS but not in PPS [12]. As the median PPS increased, the probability of detecting a statistically significant difference in OS decreased substantially. Even for a trial with an observed P value for improvement in PFS of 0.001, whereas there was a >90% probability for statistical significance of the difference in OS if the median PPS was 2 months, this probability decreased to only ~50% if the median PPS was 6 months. In the present study, we found that median PPS constituted more than half of median OS and that median PPS was >6 months in recent trials for NSCLC.

Surrogacy of PFS for OS has often been assessed by quantifying the strength of the association between these end points at the individual level (referred to as individual-level surrogacy) and of that between the effects of treatment on these

Table 2. Average median PFS, OS, and PPS as well as the average proportion of OS accounted for by PPS for trial arms in all trials or in trials according to year of completion of trial enrollment

Trials	No. of arms	No. of patients	Average median (months)			Average PPS/OS (%)
			PFS	OS	PPS	
All	151	37 986	4.9 (0.09)	10.3 (0.24)	5.4 (0.22)	50.1 (1.00)
Recent (2003 and later)	69	19 334	4.9 (0.13)	11.3 (0.42)	6.5 (0.37)	54.9 (1.31)
Older (up to and including 2002)	82	18 652	4.9 (0.13)	9.4[a] (0.17)	4.4[a] (0.16)	45.9[a] (1.33)

Values in brackets are standard errors.
[a]$P < 0.0001$ versus the corresponding value for recent trials (z test).
OS, overall survival; PFS, progression-free survival; PPS, postprogression survival; TTP, time to progression.

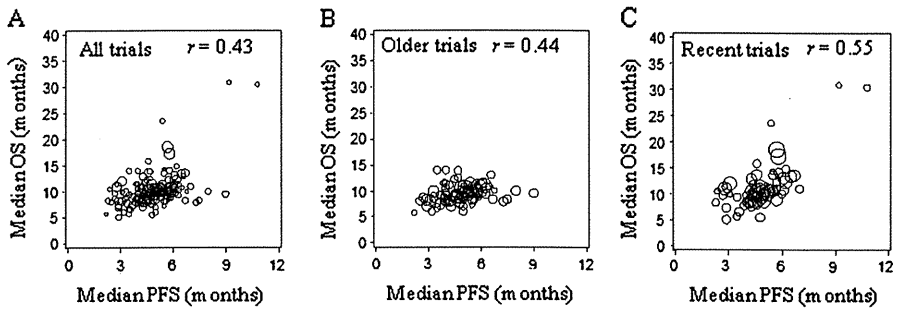

Figure 2. Relation between median overall survival (OS) and median progression-free survival (PFS) for 151 arms of 69 phase III trials for advanced non-small-cell lung cancer. (A) All trials. (B) Older trials (trial enrollment finished between 1996 and 2002). (C) Recent trials (trial enrollment finished between 2003 and 2006). The area of each circle is proportional to the number of patients in each trial arm. The *r* values represent Spearman's rank correlation coefficient.

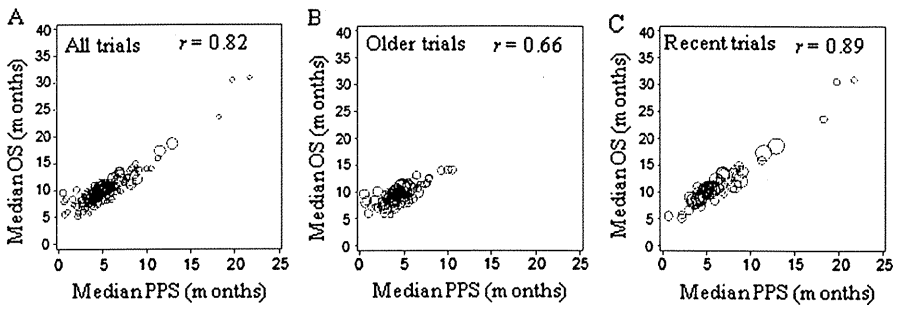

Figure 3. Relation between median overall survival (OS) and median progression-free survival (PPS) for 151 arms of 69 phase III trials for advanced non-small-cell lung cancer. (A) All trials. (B) Older trials (trial enrollment finished between 1996 and 2002). (C) Recent trials (trial enrollment finished between 2003 and 2006). The area of each circle is proportional to the number of patients in each trial arm. The *r* values represent Spearman's rank correlation coefficient.

end points (trial-level surrogacy) [18–21]. Our examination of the correlation between PFS and OS was not an exercise in surrogate validation because of the lack of investigation into the correlation between the effects of chemotherapy on these end points. However, the present study has yielded the key finding that PPS, not PFS, is highly associated with OS.

The present study has several limitations. First, our analysis was based on abstracted data. The use of individual patient data might be expected to allow a better characterization of the relation between OS and other end points based on tumor assessment, including PFS and TTP. However, such an approach would restrict the analysis to a small number of trials and would hinder its replication by independent researchers. Second, the results of our study potentially have several confounders due to selection of many heterogeneous trials for analysis. The results are generally unaccountable without appropriate adjustment for patient characteristics dependent on differences in predefined eligibility criteria for enrollment in the clinical trials. Third, the assessment of disease progression is potentially subject to measurement error and bias in individual patients, and the quality of measurement for end points based on tumor assessment can vary between centers and trials. Finally, two end points (PFS and TTP) based on tumor assessment are considered as the same parameter, following the example of a previous report for advanced breast cancer [10]. PFS is defined as the time from randomization to tumor progression or death, whereas TTP is defined similarly but considers death as a time point when censoring occurs. TTP is the same as PFS if death does not occur during treatment. Given that death rarely occurs before disease progression in advanced NSCLC, we reasonably considered PFS to be the same as TTP for our analysis. Indeed, we separately analyzed clinical trials providing PFS (n = 63 arms) or TTP (n = 88 arms), and we found a consistent association between OS and PPS (data not shown). These data thus support our approach in which these two end points (PFS and TTP) are collectively referred to as PFS in the present analysis.

As far as we are aware, our study is the first to analyze PPS in advanced NSCLC. Our findings indicate that, especially for recent trials, PPS is highly associated with OS for first-line chemotherapy in patients with advanced NSCLC, whereas PFS is only moderately associated with OS. Therefore, OS remains an appropriate end point of clinical trials for chemotherapy-naive patients with advanced NSCLC. Given the great effect of PPS on OS, we propose a precise assessment of clinical course after disease progression in each clinical trial.

funding

The study was not supported by a sponsor or funding agency.

disclosure

The authors declare no conflicts of interest.

references

1. Breathnach OS, Freidlin B, Conley B et al. Twenty-two years of phase III trials for patients with advanced non-small-cell lung cancer: sobering results. J Clin Oncol 2001; 19: 1734–1742.
2. Carney DN. Lung cancer—time to move on from chemotherapy. N Engl J Med 2002; 346: 126–128.
3. Hotta K, Matsuo K. Long-standing debate on cisplatin- versus carboplatin-based chemotherapy in the treatment of advanced non-small cell lung cancer. J Thorac Oncol 2007; 2: 96.
4. Hotta K, Matsuo K, Ueoka H et al. Meta-analysis of randomized clinical trials comparing cisplatin to carboplatin in patients with advanced non-small-cell lung cancer. J Clin Oncol 2004; 22: 3852–3859.
5. Azzoli CG, Baker S Jr, Temin S et al. American Society of Clinical Oncology Clinical Practice Guideline update on chemotherapy for stage IV non-small-cell lung cancer. J Clin Oncol 2009; 27: 6251–6266.
6. Wakelee HA, Bernardo P, Johnson DH, Schiller JH. Changes in the natural history of nonsmall cell lung cancer (NSCLC)—comparison of outcomes and characteristics in patients with advanced NSCLC entered in Eastern Cooperative Oncology Group trials before and after 1990. Cancer 2006; 106: 2208–2217.
7. Soria JC, Massard C, Le Chevalier T. Should progression-free survival be the primary measure of efficacy for advanced NSCLC therapy? Ann Oncol 2010; 21: 2324–2332.
8. Reck M, von Pawel J, Zatloukal P et al. Overall survival with cisplatin-gemcitabine and bevacizumab or placebo as first-line therapy for nonsquamous non-small-cell lung cancer: results from a randomised phase III trial (AVAiL). Ann Oncol 2010; 21: 1804–1809.
9. Reck M, von Pawel J, Zatloukal P et al. Phase III trial of cisplatin plus gemcitabine with either placebo or bevacizumab as first-line therapy for nonsquamous non-small-cell lung cancer: AVAil. J Clin Oncol 2009; 27: 1227–1234.
10. Saad ED, Katz A, Buyse M. Overall survival and post-progression survival in advanced breast cancer: a review of recent randomized clinical trials. J Clin Oncol 2010; 28: 1958–1962.
11. DerSimonian R, Laird N. Meta-analysis in clinical trials. Control Clin Trials 1986; 7: 177–188.
12. Broglio KR, Berry DA. Detecting an overall survival benefit that is derived from progression-free survival. J Natl Cancer Inst 2009; 101: 1642–1649.
13. Sandler AB, Nemunaitis J, Denham C et al. Phase III trial of gemcitabine plus cisplatin versus cisplatin alone in patients with locally advanced or metastatic non-small-cell lung cancer. J Clin Oncol 2000; 18: 122–130.
14. Fossella FV, DeVore R, Kerr RN et al. Randomized phase III trial of docetaxel versus vinorelbine or ifosfamide in patients with advanced non-small-cell lung cancer previously treated with platinum-containing chemotherapy regimens. The TAX 320 Non-Small Cell Lung Cancer Study Group. J Clin Oncol 2000; 18: 2354–2362.
15. Hanna N, Shepherd FA, Fossella FV et al. Randomized phase III trial of pemetrexed versus docetaxel in patients with non-small-cell lung cancer previously treated with chemotherapy. J Clin Oncol 2004; 22: 1589–1597.
16. Kim ES, Hirsh V, Mok T et al. Gefitinib versus docetaxel in previously treated non-small-cell lung cancer (INTEREST): a randomised phase III trial. Lancet 2008; 372: 1809–1818.
17. Shepherd FA, Rodrigues Pereira J, Ciuleanu T et al. Erlotinib in previously treated non-small-cell lung cancer. N Engl J Med 2005; 353: 123–132.
18. Buyse M, Squifflet P, Laporte S et al. Prediction of survival benefits from progression-free survival in patients with advanced non small cell lung cancer: evidence from a pooled analysis of 2,838 patients randomized in 7 trials. J Clin Oncol 2008; 26 (Suppl): (Abstr 8019).
19. Mauguen A, Michiels S, Burdett S et al. Evaluation of progression-free survival as a surrogate endpoint for overall survival when evaluating the effect of chemotherapy and radiotherapy in locally advanced lung cancer using data from four individual patient data meta-analyses. J Thorac Oncol 2011; 6 (Suppl 2): S464–S465.
20. Hotta K, Fujiwara Y, Matsuo K et al. Time to progression as a surrogate marker for overall survival in patients with advanced non-small cell lung cancer. J Thorac Oncol 2009; 4: 311–317.
21. Johnson KR, Ringland C, Stokes BJ et al. Response rate or time to progression as predictors of survival in trials of metastatic colorectal cancer or non-small-cell lung cancer: a meta-analysis. Lancet Oncol 2006; 7: 741–746.

Jpn J Clin Oncol 2011;41(9)1067–1073
doi:10.1093/jjco/hyr110
Advance Access Publication 10 August 2011

The Safety and Tolerability of Intravenous ASA404 When Administered in Combination with Docetaxel (60 or 75 mg/m^2) in Japanese Patients with Advanced or Recurrent Solid Tumors

Haruko Daga[1], Toyoaki Hida[2], Shizu Ishikawa[2], Junichi Shimizu[2], Shinya Tokunaga[1], Yoshitsugu Horio[2], Ken Kobayashi[3] and Koji Takeda[1,*]

[1]Osaka City General Hospital, Osaka, [2]Aichi Cancer Center Hospital, Aichi and [3]Novartis Pharma K.K., Tokyo, Japan

*For reprints and all correspondence: Koji Takeda, Osaka City General Hospital, 2-13-22 Miyakojimahondori, Miyakojima-ku, Osaka 534-0021, Japan. E-mail: kkk-take@ga2.so-net.ne.jp

Received May 10, 2011; accepted July 9, 2011

Objective: This Phase I study was carried out to assess the safety, tolerability, pharmacokinetics and preliminary efficacy of the flavonoid tumor-vascular disrupting agent ASA404 (vadimezan) in combination with docetaxel in Japanese patients with advanced or recurrent solid tumors.
Methods: Nine Japanese patients were given ASA404 (1800 mg/m^2) plus two doses of docetaxel, 60 or 75 mg/m^2, administered every 3 weeks.
Results: Dose-limiting toxicity of Grade 3 febrile neutropenia was observed in one patient during Cycle 1 at Level 2 of ASA404 (1800 mg/m^2) and docetaxel (75 mg/m^2) treatment. The most frequently reported adverse events were neutropenia, fatigue, alopecia, decreased appetite, constipation and injection site pain. These adverse events were mainly Grade 1 or 2 in severity and, with the exception of injection site pain, were typically associated with docetaxel therapy. A partial response was observed in one patient, and five patients (55.6%) exhibited stable disease. Overall, the study demonstrated that ASA404 has an acceptable tolerability profile when combined with docetaxel at doses up to 75 mg/m^2 in Japanese patients with advanced solid tumors.
Conclusions: The study supports the enrollment of Japanese patients in the Phase III study (ATTRACT-2) of ASA404 in combination with docetaxel for the second-line treatment of advanced non-small cell lung cancer.
Clinicaltrials.gov identifier: NCT01285453

Key words: ASA404 – vadimezan – pharmacokinetic – safety – Japanese

INTRODUCTION

The combination of the tumor-vascular disrupting agent (tumor-VDA) ASA404 (vadimezan) with taxane-based chemotherapy, such as docetaxel (DTX), is based on potential complementary properties of the two different classes of agent. ASA404-induced decreases in blood flow may lead to entrapment of a concomitantly administered drug within the tumor, and the activity of ASA404, which causes necrosis at the tumor core, may be maximized by combining it with chemotherapeutic agents, which tend to have greatest effect at the tumor periphery (1–3). Pre-clinical studies of ASA404 in combination with different chemotherapeutic agents have demonstrated enhanced antitumor activity compared with chemotherapy alone, and this effect is most striking with taxanes (1–3).

Following three Phase I clinical trials with single-agent ASA404, a dose of 1200 mg/m^2 was selected for a

randomized Phase II study in combination with DTX for prostate cancer. This study demonstrated the safety of ASA404 (1200 mg/m^2) when combined with DTX at 75 mg/m^2 (4). Another Phase II study in combination with paclitaxel and carboplatin for non-small cell lung cancer (NSCLC) demonstrated the safety and tolerability of ASA404 when administered at doses of 1200 or 1800 mg/m^2 (5,6). In Japan, a Phase I study of ASA404 (600–1800 mg/m^2) in combination with paclitaxel and carboplatin demonstrated the safety of ASA404 (1800 mg/m^2) and its preliminary efficacy profile in Japanese patients with previously untreated advanced NSCLC (7).

Although DTX is the current standard second-line chemotherapy for advanced NSCLC, its limitations as monotherapy include low response rates, brief duration of disease control and minimal survival advantage (8,9). New combination treatment regimens are therefore an urgent unmet need. A randomized, double-blind, placebo-controlled Phase III study of ASA404 (1800 mg/m^2) in combination with DTX (75 mg/m^2) as a second-line treatment of advanced NSCLC (ATTRACT-2) has been conducted (10). However, at that time, with the exception of prostate cancer, DTX was approved only at doses of 60–70 mg/m^2 in Japan (11–13). The primary objective of this open-label, non-randomized, dose-escalation Phase I study was to assess the tolerability of intravenous ASA404 (1800 mg/m^2) when administered in combination with DTX (60 or 75 mg/m^2) in Japanese patients with advanced or recurrent solid tumors. Secondary objectives were to characterize the safety profile of ASA404 + DTX in Japanese patients, to assess the pharmacokinetic (PK) profile of the combination in this patient population and to evaluate preliminary evidence of antitumor activity. The study was conducted to consider the participation of Japanese patients in a global Phase III study.

PATIENTS AND METHODS

Patient Population

Japanese patients ≥20 years of age, WHO performance status (PS) 0–1, with advanced or recurrent solid tumors were enrolled in the study. Patients had received at least one prior chemotherapeutic or hormonal regimen, excluding DTX-containing regimens. Specific criteria for exclusion were symptomatic central nervous system (CNS) metastases requiring treatment, or history of another clinically significant primary malignancy; radiotherapy within 4 weeks (within 2 weeks for palliative treatment); major surgery within 4 weeks prior to study drug exposure; pleural effusion requiring drainage; other antineoplastic therapy within 4 weeks of starting study drug treatment (6 weeks for nitrosoureas, mitomycin C and monoclonal antibodies); prior exposure to ASA404 or other tumor-VDAs; long QT syndrome; myocardial infarction within 12 months; poorly controlled angina pectoris; ventricular tachycardia; history of ventricular fibrillation or Torsades de Pointes; and use of medication known to prolong the QT interval. The study protocol was approved by the Institutional Review Board of each site, and all patients gave written informed consent for participation. The study was conducted in accordance with the Declaration of Helsinki and in accordance with the International Conference on Harmonisation guidelines on Good Clinical Practice, and applicable local regulatory requirement and laws.

Dosing and Administration

The starting dose of ASA404 was selected based on the current available results of clinical trials in western countries and in Japan. The initial DTX dose was the approved dose of 60 mg/m^2, which was then escalated to 75 mg/m^2 while keeping the dose of ASA404 constant. In principle, the dose escalation was operated using a 3 + 3 design principle with no intra-patient dose escalation, and the target dose of ASA404 1800 mg/m^2 plus DTX 75 mg/m^2 would be evaluated in six patients. The first three patients were treated with ASA404 (1800 mg/m^2 IV, 20 min infusion) in combination with DTX (60 mg/m^2 IV, 1 h infusion) on Day 1 of each cycle (21-day cycles). If no dose-limiting toxicity (DLT) was noted in the first three evaluable patients in Cycle 1 of the initial dose, the next dose of DTX (75 mg/m^2) was evaluated in combination with ASA404 (1800 mg/m^2). If DLT was observed in one of the first three patients at the initial dose level, then three patients were added to that dose level with dose-escalation proceeding if DLT was noted in one out of six patients. Planned enrollment at dose level 2 was six patients. If no further DLTs were observed, then dose escalation was to proceed to the next dose level.

Study treatment was continued until disease progression or unacceptable toxicity. Patient safety profiles and tolerability were individually assessed during Cycle 1. Dose-escalation decisions were made based on Cycle 1 data from evaluable patients according to the incidence of DLT during Cycle 1. DLTs were defined as adverse events (AEs) or abnormal laboratory values unrelated to disease, occurring before Day 21 in Cycle 1 and included hematologic toxicity (Grade 4 neutropenia for >7 consecutive days, Grade 4 thrombocytopenia, ≥Grade 3 thrombocytopenia requiring platelet transfusion, febrile neutropenia), non-hematologic toxicity (Grade 4 nausea/vomiting, fatigue or anorexia, Grade 3 CNS toxicity, Grade ≥3 other toxicity) and treatment delay of over 3 weeks. Concomitant granulocyte colony-stimulating factor was acceptable for hematologic abnormalities (neutropenia or lymphopenia) throughout the study period.

Safety Assessments

The safety population comprised all patients who had received at least one dose of ASA404 and had at least one post-baseline safety assessment after drug administration. Safety was evaluated using the assessment of AE and laboratory test data, electrocardiography at various time points (Cycle 1: prior to the start of study drug infusion, 30 min

after, 1 h after, then hourly until 4 h after, 24 h after; Cycle 2: prior to the start and 1 h after the end of infusion; end of study) and regular assessments of vital signs and physical condition. Ophthalmic evaluations were also performed by the investigator for all patients in the study. The assessment of safety was summarized descriptively for the incidence of AEs and laboratory abnormalities by severity using the Common Terminology Criteria for Adverse Events, version 3.0 (CTCAE Ver.3.0).

PK Analyses

To characterize the PK profile of ASA404, plasma concentrations of total (sum of plasma protein bound and unbound) ASA404 were measured during Cycle 1 (immediately prior to infusion, <1 min before the end of infusion, and at 0.5, 1, 2, 4, 6, 24 and 48 h time points after infusion) and Cycles 2–6 (immediately prior to infusion, <1 min before the end, and 1 and 4 h after infusion). Free (protein unbound) plasma ASA404 concentrations were also measured in Cycle 1 only. Urinary excretion was determined at Cycle 1 Day 1 (prior to infusion, start of infusion to 6 h post-infusion and 6–24 h post-infusion) and Cycle 1 Day 2 (24–48 h post-infusion). Concentrations of ASA404 in the plasma and urine were determined by liquid chromatography/tandem mass spectroscopy. PK parameters were calculated by a non-compartmental method using WinNonlin Professional Version 5.2, from the individual plasma concentration–time profiles and urinary excretion.

Efficacy Assessments

Tumor response was assessed in patients with measurable disease at baseline according to the Response Evaluation Criteria in Solid Tumors (RECIST) criteria, performed within 28 days before the start of treatment. Tumor assessment was carried out every 6 weeks and at the end of study by radiologic techniques or, if appropriate, by physical measurement. Best overall response in each patient was evaluated as complete response (CR), partial response (PR), progressive disease (PD) or stable disease (SD). The objective response rate (ORR) in the study was evaluated as the number of patients with CR or PR.

RESULTS

Accrual, Patient Characteristics and Exposure

A total of nine patients were recruited with baseline characteristics as presented in Table 1. The median age was 64

Table 1. Patient demographics and disease characteristics (full analysis set)

	ASA404 1800 mg/m^2, DTX 60 mg/m^2 ($n = 3$)	ASA404 1800 mg/m^2, DTX 75 mg/m^2 ($n = 6$)	All patients ($n = 9$)
Age (years), mean ± SD	64.3 ± 0.58	62.3 ± 7.50	63.0 ± 6.02
Sex [male, *n* (%)]	2 (66.7)	6 (100.0)	8 (88.9)
Height (cm), mean ± SD	157.3 ± 11.93	165.9 ± 7.22	163.1 ± 9.31
Weight (kg), mean ± SD	54.1 ± 13.10	66.5 ± 15.08	62.4 ± 14.95
WHO PS, *n* (%)			
0	1 (33.3)	4 (66.7)	5 (55.6)
1	2 (66.7)	2 (33.3)	4 (44.4)
Primary site of cancer, *n* (%)			
Lung	2 (66.7)	5 (83.3)	7 (77.8)
Oesophagus	0	1 (16.7)	1 (11.1)
Thymic carcinoma	1 (33.3)	0	1 (11.1)
Histology/cytology, *n* (%)			
Adenocarcinoma	0	1 (16.7)	1 (11.1)
Squamous cell carcinoma	2 (66.7)	3 (50.0)	5 (55.6)
Large cell carcinoma	0	2 (33.3)	2 (22.2)
Other	1 (33.3)	0	1 (11.1)
No. of prior chemotherapy regimens, *n* (%)			
1	1 (33.3)	4 (66.7)	5 (55.6)
2	1 (33.3)	2 (33.3)	3 (33.3)
3	1 (33.3)	0	1 (11.1)

DTX, docetaxel; PS, performance status.

years (range 48–68 years), and eight patients (88.9%) were males. The majority of patients ($n = 7$, 77.8%) had NSCLC. Five patients (55.6%) had PS = 0 at baseline and four patients had PS = 1. The most common histologic type of tumor was squamous cell carcinoma (five patients, 55.6%). Two patients had no target lesions. All patients had received prior chemotherapy and five patients (55.6%) had received one regimen. A total of nine patients were treated with ASA404 and DTX. Approximately 80% of patients received a fourth cycle of study drug treatment and the median cumulative dose was similar within each dose level (12384.0 mg ASA404 at DTX 60 mg/m^2 and 13392.0 mg ASA404 at DTX 75 mg/m^2).

Safety

All patients experienced AEs which were determined by investigators when associated with either DTX or ASA404. One patient receiving ASA404 (1800 mg/m^2) and DTX (75 mg/m^2) had a DLT of Grade 3 febrile neutropenia. The most frequently occurring (>50% for all patients) AEs were neutropenia, fatigue, alopecia, decreased appetite, constipation, injection site pain, rash, leukopenia and arthralgia (all events, regardless of suspected relationship to the study drug). The most frequently occurring Grade 3 or 4 AEs were hematologic abnormalities—neutropenia, leukopenia and febrile neutropenia (Table 2). Serious AEs suspected as related to study drugs (both ASA404 and DTX) occurred in two patients (interstitial lung disease and urinary retention), and both resolved with appropriate medical intervention.

The most frequently reported AE that was suspected to be related to only ASA404 was injection site pain, which was reported in seven patients (77.8%). Other less frequent AEs related to ASA404 treatment were injection site reaction and photophobia (reported in one patient each). The neutropenia reported in the study was quickly resolved with treatment, which included granulocyte colony-stimulating factor.

Electrocardiogram-evaluated QT prolongation occurred in one patient but was not regarded as an AE, and no AEs related to QTc prolongation were reported. No new ophthalmic abnormalities were reported in the study; three patients reported Grade 1 eye disorders of ocular hyperemia and photophobia (11.1% each)—these study drug-related events resolved rapidly without medication.

A total of seven patients were discontinued from the study due to AEs or PD. Dose reductions of DTX were required in three patients due to AEs (33.3%); all of which resolved within 10 days of dose reduction enabling study drug continuation. No deaths were recorded during the study.

Efficacy

The best objective response by investigator assessment was PR in one patient (11.1%) and SD was achieved in five patients (55.6%). There were no CR recorded in the study and two patients (22.2%) had PD.

Table 2. Frequently occurring (>30% of all patients) and Grade 3/4 adverse events regardless of study drug relationship (ASA404 or DTX) by preferred term (safety set)

Adverse events, *n* (%)	ASA404 1800 mg/m^2, DTX 60 mg/m^2 ($n = 3$)		ASA404 1800 mg/m^2, DTX 75 mg/m^2 ($n = 6$)	
	All	Grade 3/4	All	Grade 3/4
Neutropenia	3 (100.0)	3 (100.0)	6 (100.0)	6 (100.0)
Fatigue	3 (100.0)	—	6 (100.0)	—
Alopecia	3 (100.0)	—	6 (100.0)	—
Decreased appetite	3 (100.0)	—	5 (83.3)	—
Constipation	3 (100.0)	1 (33.3)	4 (66.7)	—
Injection site pain	3 (100.0)	—	4 (66.7)	—
Rash	2 (66.7)	—	4 (66.7)	—
Leukopenia	1 (33.3)	1 (33.3)	4 (66.7)	4 (66.7)
Febrile neutropenia	—	1 (33.3)	—	1 (16.7)
Hypersensitivity	—	—	—	1 (16.7)
Hyperuricemia		1 (33.3)	—	—
Arthralgia	2 (66.7)	—	3 (50.0)	—
Nausea	1 (33.3)	—	3 (50.0)	—
Myalgia	1 (33.3)	—	3 (50.0)	—
Diarrhea	2 (66.7)	—	2 (33.3)	—
Dysgeusia	1 (33.3)	—	3 (50.0)	—
Urinary retention	—	—	—	1 (16.7)
Stomatitis	1 (33.3)	—	2 (33.3)	—
Peripheral sensory neuropathy	1 (33.3)	—	2 (33.3)	—
Flushing	2 (66.7)	—	1 (16.7)	—

AEs occurring throughout the study period until 28 days after last date of drug exposure are included.

Pharmacokinetics

Mean plasma concentration–time profiles and parameters were comparable for the 60 and 75 mg/m^2 DTX doses following IV administration of DTX and ASA404 1800 mg/m^2. C_{max} and AUC of free ASA404 were ~1/20 and 1/40 of those of total ASA404, respectively. The unbound fraction decreased with time following the end of drug infusion (Table 3 and Figs 1 and 2). Renal excretion of total ASA404 48 h following intravenous administration was 2.56% (at DTX 60 mg/m^2) and 3.64% (at DTX 75 mg/m^2) of the administered dose, indicating that this is a minor pathway of elimination of ASA404 from the systemic circulation.

DISCUSSION

This single-arm, open-label study evaluated the addition of the flavonoid tumor-VDA ASA404 (1800 mg/m^2) to two doses of DTX (60 or 75 mg/m^2) in a total of nine patients,

Table 3. Pharmacokinetic parameters for ASA404

PK parameter	ASA404 1800 mg/m^2, DTX 60 mg/m^2 ($n = 3$)		ASA404 1800 mg/m^2, DTX 75 mg/m^2 ($n = 6$)	
	Total ASA404	Free ASA404	Total ASA404	Free ASA404
C_{max} (μg/ml)	282 ± 1.53	17.6 ± 4.13	280 ± 28.7	14.4 ± 3.97
t_{max} (h)	0.333 (0.333–0.833)	0.333 (0.333–0.833)	0.600 (0.317–0.833)	0.833 (0.350–0.933)
$AUC_{0-tlast}$ (h μg/ml)	1610 ± 129	45.0 ± 3.46	1580 ± 222	37.4 ± 11.1
AUC_{inf} (h μg/ml)	1650 ± 126	46.3 ± 2.49	1590 ± 227	38.0 ± 11.3
AUC_{0-24h} (h μg/ml)	1440 ± 108	43.5 ± 2.38	1470 ± 182	36.9 ± 11.1
$t_{1/2}$ (h)	9.77 ± 3.21	9.08 ± 1.85	7.17 + 0.747	5.94 ± 2.30
CL (l/h)	1.69 ± 0.355	59.8 ± 10.1	1.99 ± 0.29	89.0 ± 30.5
V_{ss} (l)	14.1 ± 1.24	310 ± 61.5	12.1 ± 1.54	327 ± 124
V_z (l)	23.2 ± 5.87	775 ± 167	20.4 ± 2.72	736 ± 284
CL_r (l/h)	0.0465 ± 0.0264	—	0.0666 ± 0.0368[a]	—
A_e (mg)	73.7 ± 38.8	—	109 ± 73.8[a]	—
f_e (%)	2.56 ± 1.07	—	3.64 ± 2.44[a]	—

Mean data ± SD. A_e, amount of ASA404 excreted in urine; $AUC_{0-tlast}$, area under the concentration–time curve from the start of ASA404 infusion to the time of the last quantifiable concentration; AUC_{inf}, AUC from start of ASA404 infusion to infinite time; AUC_{0-24h}, AUC from the start of ASA404 infusion to 24 h after the end of infusion; CL, total body clearance; CL_r, renal clearance; C_{max}, maximum plasma concentration from the start of ASA404 infusion; f_e, fractional excretion in urine; $t_{1/2}$, elimination half-life associated with the terminal slope; t_{max}, time to reach maximum concentration; V_{ss}, volume of distribution at steady state; V_z, volume of distribution during the terminal phase.
[a]$n = 5$; data from one subject excluded due to lost sample.

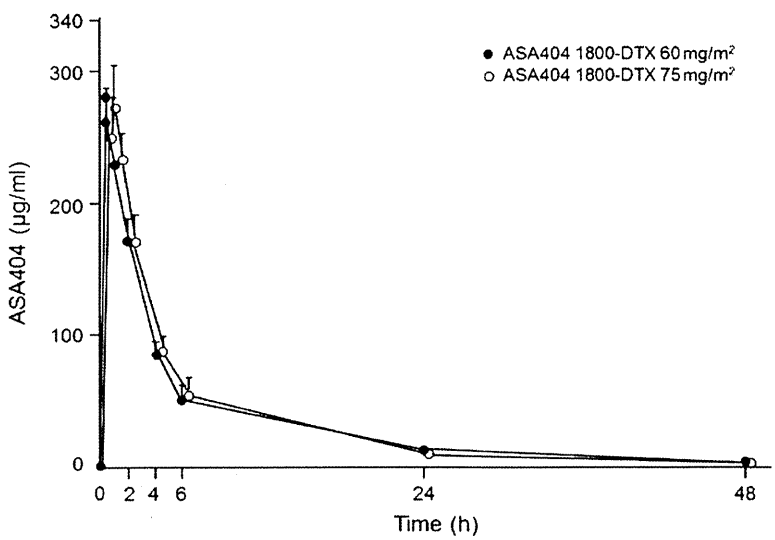

Figure 1. Mean plasma concentration–time profile of total ASA404.

of which 80% received a fourth cycle of study drug. ASA404 1800 mg/m^2 when administered in combination with DTX at dose levels of 60 and 75 mg/m^2 was therefore found to be generally safe and well tolerated in Japanese patients with advanced or recurrent solid tumors and the incidence of DLTs was less than one out of three patients. The safety profile was similar to that seen in previous studies conducted in western countries and Japan. The AEs reported in the study were mainly Grade 1 or 2 in severity, and with the exception of injection site pain, were typically those associated with DTX therapy (14).

Increasing the DTX dose from 60 to 75 mg/m^2 in combination with ASA404 did not affect the PK profile of ASA404 between the two dose levels, including its protein binding. Plasma concentrations of total ASA404 at the end of infusion and 1 h after infusion were constant through the treatment cycles, indicating that the proposed 3 weekly dosing will not result in ASA404 accumulation or induction

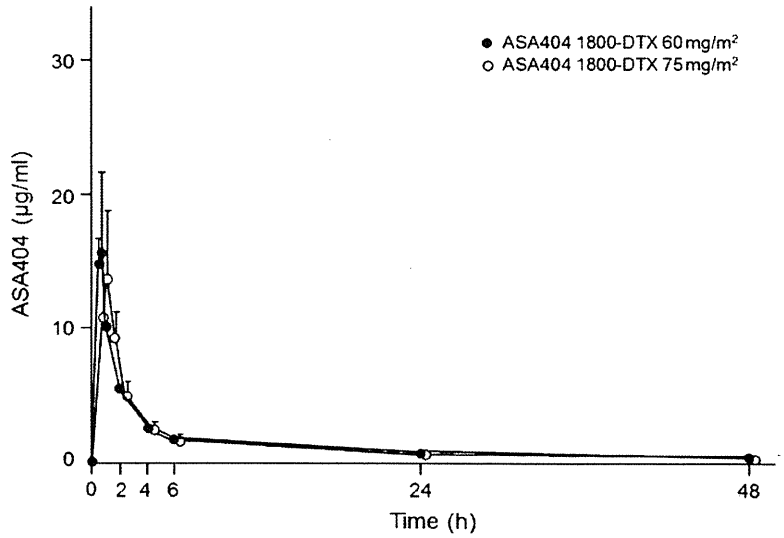

Figure 2. Mean plasma concentration–time profile of free ASA404.

of enzymes involved in ASA404 metabolic pathways. Although the influence of ASA404 on the PK profile of DTX was not evaluated in the current study, previous studies have shown that co-administration of ASA404 with DTX does not affect total systemic exposure of either drug in patients with hormone-refractory prostate cancer (4). Other studies in patients with NSCLC have also shown that ASA404 does not alter the PK profile of paclitaxel (6).

Overall, this Phase I study demonstrates that ASA404 (1800 mg/m^2) has an acceptable tolerability profile when combined with DTX at doses up to 75 mg/m^2 in Japanese patients with advanced solid tumors including NSCLC. This DTX dose was not approved in Japan at the time of the study, except for prostate cancer. This study evaluated a small analysis set, which requires confirmation in a larger randomized controlled trial; nonetheless, the data support the enrollment of Japanese patients in the Phase III study of ASA404 in combination with DTX for the second-line treatment of advanced NSCLC (ATTRACT-2). Japanese patients participated in the ATTRACT-2 study based on the results of the Phase I study; however, the Phase III study was halted following interim data analysis showing futility, even though no safety concerns were identified (15).

Acknowledgements

Medical writing assistance was provided by Articulate Science, London, UK (funded by Novartis Pharmaceuticals Corporation).

Funding

This study was supported by Novartis Pharma K.K.

Conflict of interest statement

None declared.

References

1. Kelland LR. Targeting established tumour vasculature: a novel approach to cancer treatment. *Curr Cancer Ther Rev* 2005;1:1–9.
2. Siemann DW, Mercer E, Lepler S, Rojiani AM. Vascular targeting agents enhance chemotherapeutic agent activities in solid tumor therapy. *Int J Cancer* 2002;99:1–6.
3. Siim BG, Lee AE, Shalal-Zwain S, Pruijn FB, McKeage MJ, Wilson WR. Marked potentiation of the antitumour activity of chemotherapeutic drugs by the antivascular agent 5,6-dimethylxanthenone-4-acetic acid (DMXAA). *Cancer Chemother Pharmacol* 2003;51:43–52.
4. Pili R, Rosenthal MA, Mainwaring PN, Van Hazel G, Srinivas S, Dreicer R, et al. Phase II study of the addition of ASA404 (vadimezan, 5,6-dimethylxanthenone-4-acetic acid/DMXAA) to docetaxel in castration-refractory metastatic prostate cancer. *Clin Cancer Res* 2010;16:2906–14.
5. McKeage MJ, Reck M, Jameson MB, Rosenthal MA, Gibbs D, Mainwaring PN, et al. Phase II study of ASA404 (vadimezan, 5,6-dimethylxanthenone-4-acetic acid/DMXAA) 1800 mg/m^2 combined with carboplatin and paclitaxel in previously untreated advanced non-small cell lung cancer. *Lung Cancer* 2009;65:192–7.
6. McKeage MJ, von Pawel J, Reck M, Jameson M, Rosenthal M, Sullivan R, et al. Randomised phase II study of ASA404 combined with carboplatin and paclitaxel in previously untreated advanced non-small cell lung cancer. *Br J Cancer* 2008;99:2006–12.
7. Hida T, Tamiya M, Nishio M, Yamamoto N, Hirashima T, Horai T, et al. Phase I study of intravenous ASA404 (vadimezan) administered in combination with paclitaxel and carboplatin in Japanese patients with non-small cell lung cancer. *Cancer Sci* 2011;102:845–51.
8. Fossella F, DeVore R, Kerr R, Crawford J, Natale R, Dunphy F, et al. Randomized phase III trial of docetaxel versus vinorelbine or ifosfamide in patients with advanced non-small cell lung cancer previously treated with platinum containing chemotherapy regimens; the TAX320 Non-Small Cell Lung Cancer Study Group. *J Clin Oncol* 2000;18:2354–62.
9. Shepherd F, Dancey J, Ramlau R, Mattson K, Gralla R, O'Rourke M, et al. Prospective randomized trial of docetaxel versus best supportive care in patients with non-small cell lung cancer previously treated with platinum-based chemotherapy. *J Clin Oncol* 2000;18:2095–103.

10. ATTRACT-2 (NCT00738387). A Phase III, randomized, double-blind, placebo-controlled multi-center study of ASA404 in combination with docetaxel in second-line treatment of patients with locally advanced or metastatic (Stage IIIb/IV) non-small cell lung cancer (NSCLC). http://clinicaltrials.gov/ct2/show/NCT00738387?term=ASA404+NSCLC&rank=2
11. Iwao-Koizumi K, Matoba R, Ueno N, Jin Kim S, Ando A, Miyoshi Y, et al. Prediction of docetaxel response in human breast cancer by gene expression profiling. *J Clin Oncol* 2010;23:422–31.
12. Naito S, Tsukamoto T, Koga H, Harabayashi T, Sumiyoshi Y, Hoshi S, et al. Docetaxel plus prednisolone for the treatment of metastatic hormone-refractory prostate cancer: a multicenter phase II trial in Japan. *Jpn J Clin Oncol* 2008;38:365–72.
13. Takeda K, Negoro S, Tamura T, Nishiwaki Y, Kudoh S, Yokota S, et al. Phase III trial of docetaxel plus gemcitabine versus docetaxel in second-line treatment of non-small cell lung cancer: results of a Japan Clinical Oncology Group trial (JCOG0104). *Ann Oncol* 2009;20:835–41.
14. Eisenhauer E, Vermorken J. The taxoids: comparative clinical pharmacology and therapeutic potential. *Drugs* 1998;55:5–30.
15. ATTRACT-2. http://www.attractstudy.com/attract-2-researching-ASA404-in-cancer-treatment.jsp.

Small-cell lung carcinoma with long-term survival: A case report

KAZUMI NISHINO[1], FUMIO IMAMURA[1], TORU KUMAGAI[1], JUNJI UCHIDA[1], YUKI AKAZAWA[1], TAKAKO OKUYAMA[1] and YASUHIKO TOMITA[2]

[1]Department of Thoracic Oncology; [2]Institute of Pathology, Osaka Medical Center for Cancer and Cardiovascular Diseases, Osaka 537-8511, Japan

Received March 28, 2011; Accepted June 20, 2011

DOI: 10.3892/ol.2011.355

Abstract. Small-cell lung carcinoma is the most aggressive among lung cancer subtypes, has a poor prognosis and is highly associated with smoking. We present a case of small-cell lung carcinoma in a patient who had never smoked and has survived for 14 years without achieving a complete remission since the first relapse. His long-term survival may be ascribed to the slow growth of the cancer cells, limited metastasis and favorable responses to the treatments he has received. During these 14 years, only two lymph node metastases and a single metastasis to the brain developed. His small-cell lung carcinoma has been well controlled each time by the various treatments he has received, including chemotherapy, radiotherapy and surgery. Pathologically, the tumor was a typical small-cell lung carcinoma with extensive necrosis. Results showed the mitotic rate and the cell proliferation markers to be greater than those in the intermediate-grade atypical carcinoid, but relatively low. Thus, we conclude that this case belongs to an overlap between intermediate- and high-grade neuroendocrine tumors.

Introduction

The 2004 World Health Organization (WHO) classification proposed four subtypes of pulmonary neuroendocrine (NE) tumors: low-grade typical carcinoid (TC), intermediate-grade atypical carcinoid (AC) and two high-grade tumors, large cell neuroendocrine carcinoma (LCNEC) and small-cell lung carcinoma (SCLC) (1). SCLC is a highly aggressive cancer and results in mortality in 2-4 months without treatment. Most patients respond to primary therapy, but survival remains poor and median survival times are reported to be approximately 24 months in limited disease and 12 months in extensive disease (2,3). In this study, we present a case of SCLC in a never smoker who has survived for 14 years without achieving a complete remission following the initial relapse.

Correspondence to: Dr Kazumi Nishino, Department of Thoracic Oncology, Osaka Medical Center for Cancer and Cardiovascular Diseases, 1-3-3 Nakamichi, Higashinari-ku, Osaka 537-8511, Japan
E-mail: nishinishipptruth@yahoo.co.jp

Key words: small-cell lung carcinoma, pulmonary neuroendocrine tumors, atypical carcinoid, The 2004 WHO Classification, long-term survival

Case report

In November 1996, a 44-year-old male, with no history of smoking, presented at the Osaka Medical Center for Cancer and Cardiovascular Diseases with an abnormal hilar shadow in the left lung, complaining of cough and dyspnea. A computerized tomography (CT) scan revealed a 4.5x3.0 cm hilar mass in the left lung (Fig. 1A). The patient was cytologically diagnosed with SCLC by bronchoscopic examination (Fig. 1B). Metastatic workup demonstrated that he had limited disease, cT2aN2M0 stage IIIA (the 7th edition of the TNM system for lung cancer). The values of serum neuron-specific enolase and carcinoembryonic antigen were within normal limits and the pro-gastrin-releasing-peptide (ProGRP) was not measured at the time. The patient received four cycles of chemotherapy consisting of cisplatin (CDDP) and etoposide, with concurrent thoracic radiation of 44 Gy at 2.2 Gy/fraction daily. The treatment resulted in a complete response. Prophylactic cranial irradiation was not performed since there was no evidence to recommend it at the time (4).

The patient remained asymptomatic and no sign of disease recurrence was detected until December 1998, when right mandibular lymphadenopathy was evidenced. By that time, the level of ProGRP had gradually been elevating from 25 pg/ml in October 1997 to 76 pg/ml in August 1998 and 133 pg/ml in December 1998 (normal range 0-45 pg/ml). Aspiration needle cytology of the lymph node revealed metastasis of SCLC, leading to the diagnosis of recurrence of SCLC as the cancer cells obtained from the lymph node revealed almost the same morphological features as the primary lung tumor cells. Since imaging studies showed no recurrence with the exception of the lesion, and the WBC count was ~3,000/μl, the patient was administered palliative radiotherapy with a total dose of 70 Gy without chemotherapy. The lymphadenopathy disappeared and the level of ProGRP decreased to 14.1 pg/ml. Two years later, in April 2000, the right axillary lymph node was found to be enlarged and cytology revealed metastasis of SCLC. Palliative radiotherapy with a total dose of 60 Gy was administered to the lesion. The lymph node swelling did not disappear completely, but the level of ProGRP decreased from 154 to 44 pg/ml. Although the level of ProGRP was slowly

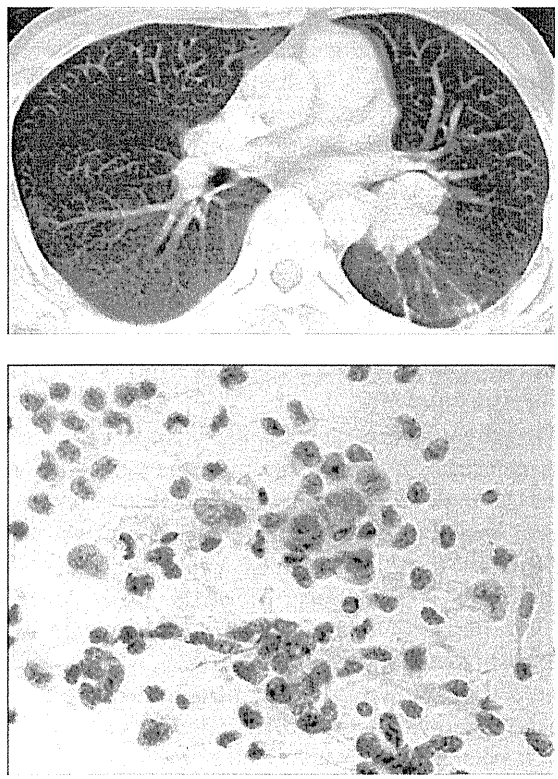

Figure 1. (A) A CT image in November 1996 revealed a 4.5x3.0-cm hilar mass in the left lung. (B) Cytology of the material obtained bronchoscopically from the primary lung tumor revealed SCLC.

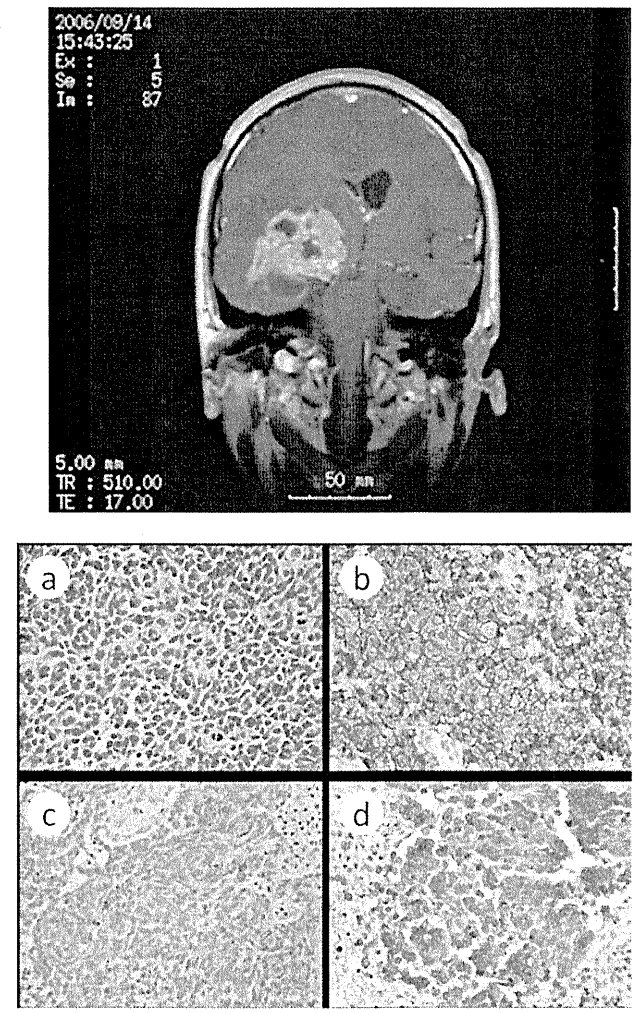

Figure 2. (A) Brain MRI in September 2006 showed a huge mass in the right temporal lobe. (B) Hematoxylin and eosin (H&E) and immunohistological staining of the specimen from the resected brain tumor. The tumor cells were positive for CD56, chromogranin and synaptophysin, indicating the neuroendocrine origin of the tumor. a, H&E stain; b, CD56 stain; c, chromogranin stain; d, synaptophysin stain. Original magnification, x200.

elevated to 150 pg/ml in November 2002, the patient observed no further symptoms and subsequently stopped consultation with the hospital.

The patient presented at the Osaka Medical Center for Cancer and Cardiovascular Diseases again in September 2006. Neurological examinations at admission indicated cerebral abnormality: left upper 1/4 homonymous hemianopsia and dysrhythmia on the electroencephalogram. The level of ProGRP was markedly elevated (2,860 pg/ml). Magnetic resonance imaging (MRI) of the brain revealed a huge mass in the right temporal lobe (Fig. 2A). The brain tumor was completely excised and histopathological examination determined it to be a metastasis of SCLC. The tumor was cytologically identical to the primary lung cancer, showing extensive necrosis, a high nuclear-to-cytoplasmic ratio and fine nuclear chromatin. The mitotic rate was 14 mitoses per 10 high-power fields (HPF) in this resected specimen. The Ki-67 labeling index was 25%. Immunohistochemical stains were positive for NE markers, including chromogranin A, synaptophysin and CD56 (Fig. 2B). The primary hilar tumor in the left lung and the right axillary lymph node revealed an increased uptake of fludeoxyglucose in positron emission tomography (PET) scanning. The patient received whole brain radiation therapy (WBRT) (30 Gy in 10 fractions), followed by systemic chemotherapy with CDDP and irinotecan hydrochloride (CPT11). Although the doses of CDDP and CPT11 were reduced to 50 and 50 mg/m^2, respectively, ProGRP levels decreased notably to 90.7 pg/ml, following chemotherapy.

From September 2007, the level of ProGRP was again gradually elevated. Recurrence of brain metastasis was detected on the MRI in November 2008 and the patient underwent intensity-modulated radiotherapy (IMRT) for the brain tumor. Following IMRT, the patient was administered chemotherapy with CDDP and CPT11. However, compliance to the chemotherapy was poor due to hematological toxicity. In September 2009, the patient was admitted for obstructive pneumonia in the left lower lobe with high fever, and treated successfully with antibiotics. The level of ProGRP elevated to 724 pg/ml and distinct progression of the primary hilar tumor in the left lung was again detected by CT. The patient refused to complete systemic chemotherapy and was followed up for 1 year. In November 2010, CT and PET detected distinct progression of the primary lung tumor resulting in atelectasis of the left lower lobe and right axillary lymphadenopathy. The level of ProGRP was elevated to 1,640 pg/ml. Chemotherapy with amrubicin was administered in December 2010.

At present, the clinical course of the patient has continued for 14 years following the initial diagnosis of SCLC and 4 years following the diagnosis of brain metastasis. The brain remains relapse-free at present. The patient is currently

continuing treatment with amrubicin for SCLC and his performance remains positive.

Discussion

NE tumors represent approximately 20% of all primary lung neoplasms (5). NE tumors of the lung are separated into four subgroups: low-grade TC, intermediate-grade AC and two high-grade malignancies, LCNEC and SCLC, according to WHO in 2004 (1). SCLC is the most common NE tumor (20% of total lung cancers), followed by LCNEC (3%), TC (2%) and AC (0.2%) (6). The tumors differ morphologically, immunohistochemically and structurally. The WHO classification defines SCLC as a NE tumor with greater than 10 mitoses/10 HPF and small-cell cytologic features. TC is considered a NE tumor with carcinoid morphology, fewer than 2 mitoses/10 HPF and lacking in necrosis, while AC is defined as a NE tumor with carcinoid morphology showing 2-10 mitoses/10 HPF or necrosis (1). The grade of malignancy of each NE subtype is correlated with clinicopathological behavior and prognosis of the disease. TC and AC are relatively slow-growing tumors and generally exhibit a favorable outcome, while LCNEC and SCLC are very aggressive with a dismal prognosis (5,6).

The accurate differential diagnosis of carcinoids from SCLC is critical in the selection of the appropriate treatment. Usually, SCLC is rarely mistaken for carcinoids, with the exception of small biopsy materials. There are also certain differences in the clinical background and profiles according to the subgroup of NE tumors. Unlike carcinoids, SCLC is markedly associated with a history of smoking (7,8). Carcinoids tend to occur in younger patients (mean age 45-50 years), whereas the high-grade NE tumors affect older patients (mean age 65 years). The former are capable of distant metastases in less than 20% of cases (most commonly to liver and bones), and SCLC tends to metastasize to the brain, liver, adrenal glands and bone with higher frequency (5,6). Due to the low response rates for chemo- and radiotherapy, surgical resection is primarily used in the treatment of carcinoids, whereas the standard treatment for limited-stage SCLC includes combined chemoradiotherapy due to high sensitivity.

This case was initially diagnosed as SCLC in 1996 by cytological sampling obtained using bronchoscopy. The initial chemoradiotherapy resulted in a complete response. Ten years later, a metastatic brain tumor was excised. Although the clinical course was not typical for SCLC, the histopathological features of the resected tumor confirmed the diagnosis of SCLC due to the morphology of the tumor cells, the positive staining with neuroendocrine markers and the 14 mitoses/10 HPF with extensive necrosis (according to the WHO classification in 2004). The Ki-67 proliferative index has recently been considered to be useful in distinguishing between the various subtypes of NE tumors, particularly in small biopsy and cytology specimens. The Ki-67 proliferation rate of TC is less than 2% and AC is less than 20% (typical rate ~10%), while the two high-grade NE tumors are higher than 20% (typical rate for SCLC is 60-100%) (6,9,10). The Ki-67 index of this case was 25%.

The clinical manifestations of this case, such as slow-growing tumors, limited metastatic potential and a favorable prognosis, with an over 14-year survival, support the diagnosis of AC, while the morphological, immunohistochemical and structural features of the tumors are typical of SCLC. We believe that this case fits the diagnostic criteria of SCLC according to the WHO classification, but it is a borderline case between AC and SCLC. Asamura *et al* reported that 5-year survival rates for TC, AC, LCNEC and SCLC in Japanese surgical cases of NE tumors were 96.2, 77.8, 40.3 and 35.7%, respectively (8). An analysis of Japanese lung cancer patients registered in 2002 revealed that SCLC accounted for 9.2% of new lung cancer cases in Japan, and 5-year survival rates were 17.2% for stage IIIA, 12.4% for stage IIIB, 3.8% for stage IV and 14.7% overall (11).

The prognosis is particularly dismal in SCLC patients with brain metastasis. In the practice guidelines recently published in the Journal of Neurooncology, the authors recommend surgical resection followed by WBRT for newly-diagnosed single brain metastases, which improves outcomes when compared to WBRT alone. However, these authors indicate that the recommendation does not apply to relatively radiosensitive tumors such as SCLC (12). By contrast, Jesien-Lewandowicz *et al* assert that patients with solitary brain metastasis from SCLC should be treated radically, in particular those at younger ages with a small primary tumor in the lung, good performance status and lack of systemic dissemination (13). Four case reports describe excellent long-term survival following resection of a solitary metastatic brain tumor of SCLC and adjuvant WBRT (13-16). In the present case, surgical resection followed by WBRT and chemotherapy was successful. Imai *et al* suggest that a subtype of slow-growing SCLC, which shows different biological properties, should be distinguished from the common type SCLC (16). Although unusual, patients with this subtype of NE tumor may potentially achieve longer survival than those with typical SCLC, and should be treated with local and multimodality treatment on a case-by-case basis.

In conclusion, we present a case report of a SCLC patient who has survived for 14 years following initial diagnosis with persistent disease, in spite of repetitive multimodality therapies. This case suggests the existence of borderline cases between intermediate- and high-grade NE tumors, and that long-term survival may be expected with suitable treatments. A method should be established to select SCLC patients with a favorable prognosis, such as this case, and to find optimal therapeutic approaches for such patients.

References

1. Beasley MB, Brambilla E and Travis WD: The 2004 World Health Organization classification of lung tumors. Semin Roentgenol 40: 90-97, 2005.
2. Jackman DM and Johnson BE: Small-cell lung cancer. Lancet 366: 1385-1396, 2005.
3. El Maalouf G, Rodier JM, Faivre S and Raymond E: Could we expect to improve survival in small cell lung cancer? Lung Cancer 57 (Suppl 2): 30-34, 2007.
4. Auperin A, Arriagada R, Pignon JP, *et al*: Prophylactic cranial irradiation for patients with small-cell lung cancer in complete remission. Prophylactic cranial irradiation overview collaborative group. N Engl J Med 341: 476-484, 1999.
5. Gustafsson BI, Kidd M, Chan A, Malfertheiner MV and Modlin IM: Bronchopulmonary neuroendocrine tumors. Cancer 113: 5-21, 2008.

6. Rekhtman N: Neuroendocrine tumors of the lung: an update. Arch Pathol Lab Med 134: 1628-1638, 2010.
7. Ou SH, Ziogas A and Zell JA: Prognostic factors for survival in extensive stage small cell lung cancer (ed-sclc): the importance of smoking history, socioeconomic and marital statuses, and ethnicity. J Thorac Oncol 4: 37-43, 2009.
8. Asamura H, Kameya T, Matsuno Y, *et al*: Neuroendocrine neoplasms of the lung: a prognostic spectrum. J Clin Oncol 24: 70-76, 2006.
9. Aslan DL, Gulbahce HE, Pambuccian SE, Manivel JC and Jessurun J: Ki-67 immunoreactivity in the differential diagnosis of pulmonary neuroendocrine neoplasms in specimens with extensive crush artifact. Am J Clin Pathol 123: 874-878, 2005.
10. Pelosi G, Rodriguez J, Viale G and Rosai J: Typical and atypical pulmonary carcinoid tumor overdiagnosed as small-cell carcinoma on biopsy specimens: a major pitfall in the management of lung cancer patients. Am J Surg Pathol 29: 179-187, 2005.
11. Sawabata N, Asamura H, Goya T, Mori M, Nakanishi Y, Eguchi K, Koshiishi Y, Okumura M, Miyaoka E and Fujii Y: Japanese lung cancer registry study: first prospective enrollment of a large number of surgical and nonsurgical cases in 2002. J Thorac Oncol 5: 1369-1375, 2010.
12. Gaspar LE, Mehta MP, Patchell RA, *et al*: The role of whole brain radiation therapy in the management of newly diagnosed brain metastases: a systematic review and evidence-based clinical practice guideline. J Neurooncol 96: 17-32, 2010.
13. Jesien-Lewandowicz E, Spych M, Fijuth J and Kordek R: Solitary brain metastasis of an occult and stable small-cell lung cancer in a schizophrenic patient: a 3-year control. Lung Cancer 69: 245-248, 2010.
14. Abratt RP, de Groot M and Willcox PA: Resection of a solitary brain metastasis in a patient with small cell lung cancer – long-term survival. Eur J Cancer 31A: 419, 1995.
15. Harrison ML and Goldstein D: Prolonged survival in a patient with an occult primary small-cell lung cancer and a solitary brain metastasis at diagnosis. Intern Med J 32: 621-622, 2002.
16. Imai R, Hayakawa K, Sakurai H, Nakayama Y, Mitsuhashi N and Niibe H: Small cell lung cancer with a brain metastasis controlled for 5 years: a case report. Jpn J Clin Oncol 31: 116-118, 2001.

CANCER

Activation of ERBB2 Signaling Causes Resistance to the EGFR-Directed Therapeutic Antibody Cetuximab

Kimio Yonesaka,[1,2,3,4] Kreshnik Zejnullahu,[1,2] Isamu Okamoto,[3] Taroh Satoh,[3] Federico Cappuzzo,[5] John Souglakos,[6,7] Dalia Ercan,[1,2] Andrew Rogers,[1,2] Massimo Roncalli,[5] Masayuki Takeda,[3] Yasuhito Fujisaka,[3] Juliet Philips,[2] Toshio Shimizu,[3] Osamu Maenishi,[8] Yonggon Cho,[9] Jason Sun,[1,2] Annarita Destro,[5] Koichi Taira,[10] Koji Takeda,[10] Takafumi Okabe,[1,2] Jeffrey Swanson,[1,2] Hiroyuki Itoh,[8] Minoru Takada,[11] Eugene Lifshits,[12] Kiyotaka Okuno,[13] Jeffrey A. Engelman,[12] Ramesh A. Shivdasani,[2,14] Kazuto Nishio,[15] Masahiro Fukuoka,[4,11] Marileila Varella-Garcia,[9] Kazuhiko Nakagawa,[3]*† Pasi A. Jänne[1,2,14]*†

Cetuximab, an antibody directed against the epidermal growth factor receptor, is an effective clinical therapy for patients with colorectal, head and neck, and non–small cell lung cancer, particularly for those with *KRAS* and *BRAF* wild-type cancers. Treatment in all patients is limited eventually by the development of acquired resistance, but little is known about the underlying mechanism. Here, we show that activation of ERBB2 signaling in cell lines, either through *ERBB2* amplification or through heregulin up-regulation, leads to persistent extracellular signal–regulated kinase 1/2 signaling and consequently to cetuximab resistance. Inhibition of ERBB2 or disruption of ERBB2/ERBB3 heterodimerization restores cetuximab sensitivity in vitro and in vivo. A subset of colorectal cancer patients who exhibit either de novo or acquired resistance to cetuximab-based therapy has *ERBB2* amplification or high levels of circulating heregulin. Collectively, these findings identify two distinct resistance mechanisms, both of which promote aberrant ERBB2 signaling, that mediate cetuximab resistance. Moreover, these results suggest that ERBB2 inhibitors, in combination with cetuximab, represent a rational therapeutic strategy that should be assessed in patients with cetuximab-resistant cancers.

INTRODUCTION

Cetuximab, an epidermal growth factor receptor (EGFR)–directed antibody, is an effective treatment alone or in combination with chemotherapy for patients with colorectal cancer (CRC), head and neck squamous cell cancer (HNSCC), and non–small cell lung cancer (NSCLC) (*1–3*). Cetuximab functions by blocking ligand binding to the extracellular domain (ECD) of EGFR, thus preventing ligand-mediated EGFR signaling. In addition, cetuximab enhances receptor internalization and degradation and induces antibody-dependent cell-mediated cytotoxicity (*4*).

In patients with CRC, the initial clinical benefits of cetuximab are variable, and not all studies demonstrate a significant improvement in progression-free survival (PFS) or overall survival (OS) with cetuximab-based therapy (*5, 6*). Prompted by these clinical observations and an increased understanding of EGFR signaling, several studies have evaluated the impact of oncogenic mutations in the EGFR signaling pathway on the efficacy of cetuximab in patients with metastatic CRC. Aberrant activation of downstream signaling pathways, especially those that result in activation of extracellular signal–regulated kinase 1/2 (ERK1/2) signaling, results in de novo clinical resistance to cetuximab-based therapy. These include mutations in *KRAS*, *BRAF*, and *NRAS* (*5–10*). Most, if not all, of the clinical benefits of cetuximab are limited to patients whose cancers do not harbor these oncogenic mutations (*11*). However, even among this molecularly enriched subset of patients, cetuximab is not uniformly clinically effective, suggesting that there are other, yet undefined, mechanisms of de novo cetuximab resistance (*5–9*). Identification of these additional resistance mechanisms may help further refine the subset of CRC patients likely to benefit from cetuximab or cetuximab-based combination therapies. In addition, although studies of genomic alterations in the EGFR signaling pathway can define the appropriate patient population to treat with a cetuximab-based regimen, all patients will ultimately develop resistance (acquired resistance) to cetuximab or other therapeutic EGFR antibodies. An understanding of acquired resistance mechanisms may help to identify effective therapies or guide the use of therapeutic combinations for patients who develop clinical cetuximab resistance. This strategy has been successful in studies of other molecular targeted therapies including EGFR kinase inhibitors (*12*).

To define additional mechanisms of de novo cetuximab resistance and to identify mechanisms of acquired cetuximab resistance, we generated and studied a series of cetuximab-resistant cell lines in vitro and in vivo. We combined our findings with studies of tumor specimens from cetuximab-treated CRC patients.

[1]Lowe Center for Thoracic Oncology, Dana-Farber Cancer Institute, Boston, MA 02215, USA. [2]Department of Medical Oncology, Dana-Farber Cancer Institute, Boston, MA 02215, USA. [3]Department of Medical Oncology, Kinki University School of Medicine, Osaka 589-8511, Japan. [4]Department of Medical Oncology, Izumi Municipal Hospital, Osaka 594-0071, Japan. [5]Istituto Clinico Humanitas, Rozzano 20089, Italy. [6]Laboratory of Tumor Biology, Medical School, University of Crete, Heraklion 71110, Greece. [7]University Hospital of Heraklion, Heraklion 71110, Greece. [8]Department of Pathology, Kinki University School of Medicine, Osaka 589-8511, Japan. [9]University of Colorado Cancer Center, Aurora, CO 80045, USA. [10]Department of Clinical Oncology, Osaka City General Hospital, Osaka 534-0021, Japan. [11]Department of Medical Oncology, Kinki University School of Medicine, Sakai Hospital, Osaka 590-0132, Japan. [12]Massachusetts General Hospital Cancer Center, Boston, MA 02129, USA. [13]Department of Surgery, Kinki University School of Medicine, Osaka 589-8511, Japan. [14]Department of Medicine, Brigham and Women's Hospital and Harvard Medical School, Boston, MA 02115, USA. [15]Department of Genome Biology, Kinki University School of Medicine, Osaka 589-8511, Japan.
*These authors contributed equally to this work.
†To whom correspondence should be addressed. E-mail: nakagawa@med.kindai.ac.jp (K.N.); pjanne@partners.org (P.A.J.)

RESULTS

ERBB2 amplification mediates cetuximab resistance

We first generated cetuximab-resistant HCC827 cells using previously described methods (*12*, *13*). We exposed cetuximab-sensitive HCC827 cells to increasing drug concentrations starting at 100 ng/ml, which is below the IC_{50} (mean inhibitory concentration), until they were able to proliferate freely in cetuximab (100 μg/ml), similar to the maximal serum concentration observed in phase 1 studies (*14*, *15*). Four independent cetuximab-resistant clones were confirmed to have lost drug sensitivity (Fig. 1A). Unlike in the parental HCC827 cells, cetuximab did not fully inhibit phospho-ERK1/2 (pERK1/2) (Fig. 1B). However, the resistant HCC827 cells remained sensitive to the EGFR kinase inhibitor gefitinib (fig. S1A), which inhibited AKT and ERK1/2 phosphorylation and resulted in apoptosis (Fig. 1B and fig. S1B). Cetuximab treatment of HCC827 cells induced G_1-S arrest, consistent with down-regulation of pERK1/2, rather than phospho-AKT (pAKT), and lack of apoptosis (Fig. 1B and fig. S1B).

Genome-wide copy number analyses comparing HCC827 cetuximab-resistant cells with parental HCC827 cells (*12*, *16*) revealed a few small

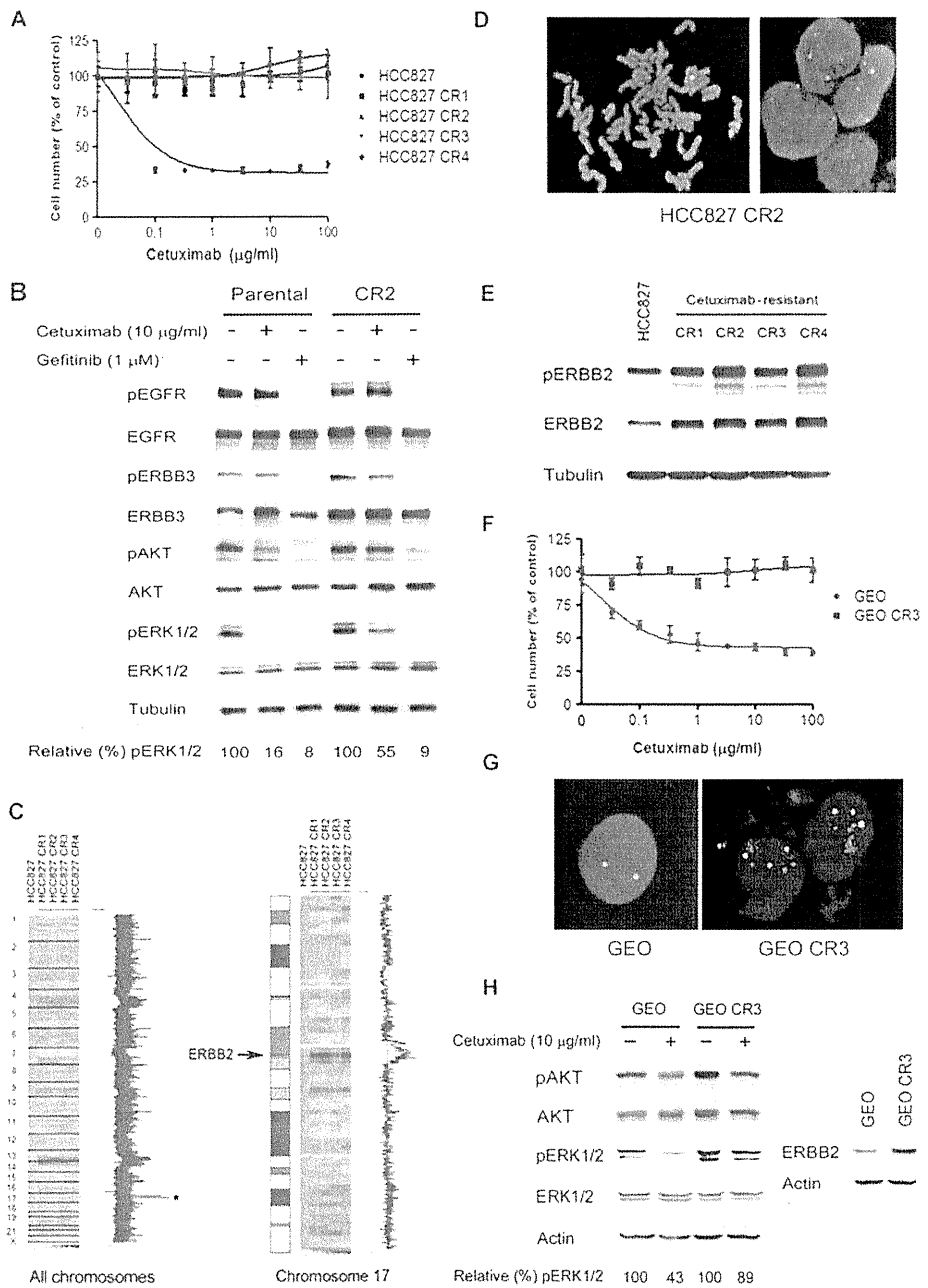

Fig. 1. Cetuximab-resistant NSCLC and CRC cells maintain ERK1/2 signaling and contain an *ERBB2* amplification. (**A**) Parental and resistant HCC827 cetuximab-resistant (CR) cells were treated with cetuximab at the indicated concentrations, and viable cells were measured after 72 hours of treatment and plotted (mean ± SD) relative to untreated controls. (**B**) Parental HCC827 and CR2 cells were treated with cetuximab (10 μg/ml) or gefitinib (1 μM) for 6 hours. Cell extracts were immunoblotted to detect the indicated proteins. (**C**) Amplification on chromosome 17 encompassing the *ERBB2* locus (asterisk, HCC827 cetuximab-resistant cells). The HCC827 cetuximab-resistant clones (right) were compared with parental HCC827 cells (first column). The blue curve on the right indicates degree of amplification of each SNP from 0 (left) to 8 (right). Left, genome-wide view; right, chromosome 17. (**D**) Metaphase (left) and interphase (right) FISH on HCC827 CR2 cells using ERBB2 (red) and CEP17 (green) probes. The HER2/CEP17 ratio was 4.7. (**E**) Expression of pERBB2 and ERBB2 in HCC827 and cetuximab-resistant cells. Cell extracts were immunoblotted to detect the indicated proteins. (**F**) Parental and resistant GEO CR3 cells were treated with cetuximab at the indicated concentrations, and viable cells were measured after 72 hours of treatment and plotted (mean ± SD) relative to untreated controls. (**G**) Interphase FISH on GEO and GEO CR3 cells using ERBB2 (red) and CEP17 (green) probes. HER2/CEP17 ratio >2 was observed in 50% of GEO CR3 cells. (**H**) (Left) Parental GEO and CR3 cells were treated with cetuximab (10 μg/ml) for 6 hours. Cell extracts were immunoblotted to detect the indicated proteins. (Right) Expression of ERBB2 in GEO and GEO CR3 cells.

changes and a larger region of copy number gain on chromosome 17 (Fig. 1C), encompassing the *ERBB2* oncogene (Fig. 1C). Amplification in *ERBB2* was confirmed with fluorescence in situ hybridization (FISH; Fig. 1D), and the HCC827 cetuximab-resistant cells expressed higher levels of both total ERBB2 and phospho-ERBB2 (pERBB2) than the parental HCC827 cells (Fig. 1E).

HCC827 cells are an NSCLC cell line. Thus, we also determined whether *ERBB2* amplification also occurred in CRC, where cetuximab is in widespread clinical use, as a result of cetuximab exposure. We generated cetuximab-resistant clones of the GEO CRC cell line (Fig. 1F) and isolated seven independent resistant clones (fig. S1C). Three of the seven clones (CR3, CR7, and CR9) harbored evidence of *ERBB2* amplification (Fig. 1G and fig. S1C). Similar to the HCC827 cetuximab-resistant cells, the GEO CR3 cells expressed increased levels of ERBB2, and cetuximab did not effectively down-regulate pERK1/2 in these cells (Fig. 1H).

To determine whether ERBB2 plays a causal role in cetuximab resistance, we depleted *ERBB2* in the HCC827 cetuximab-resistant cells using an ERBB2-specific short hairpin RNA (shRNA), which restored both cetuximab sensitivity and its ability to down-regulate pERK1/2 (Fig. 2A). Furthermore, the combination of an ERBB2 antibody, trastuzumab, with cetuximab inhibited the growth of HCC827 CR2 (Fig. 2B) and GEO CR3 cells (Fig. 2C) compared to either agent alone. Treatment with the ERBB2 kinase inhibitor lapatinib restored sensitivity of HCC827 cetuximab-resistant cells to cetuximab (fig. S4A), and cetuximab was able to inhibit pERK1/2 in the presence of lapatinib (fig. S4B). Because lapatinib also inhibits EGFR, we introduced either a wild-type or a kinase-dead (K753M) *ERBB2* into HCC827 cells (Fig. 2D) to formally determine the requirement for ERBB2 kinase activity in mediating cetuximab resistance. ERBB2 K753M did not cause resistance to cetuximab (Fig. 2D), and cetuximab still inhibited ERK1/2 signaling in these cells (Fig. 2E). Collectively, these findings suggest that *ERBB2* amplification is the principal mechanism of resistance to cetuximab in both NSCLC and CRC cells and that inhibition of ERBB2, in conjunction with cetuximab, represents a potential treatment strategy for patients with acquired cetuximab resistance.

ERBB2 amplification activates ERK1/2 signaling to mediate cetuximab resistance

To further evaluate whether ERBB2 could confer resistance in other cetuximab-sensitive cells, we used the HNSCC cell line HN11 and the NSCLC cell line H1648, both cetuximab-sensitive in vitro (*17*). Introduction of *ERBB2* to the cells conferred resistance to cetuximab in HCC827, HN11, and H1648 cells (Fig. 2F and fig. S2). In addition, cetuximab was unable to down-regulate pERK1/2 in either HCC827 or HN11 cells overexpressing ERBB2, in contrast to control green fluorescent protein (GFP)–infected cells (Fig. 2G and fig. S3A). Because *ERBB2* amplification could potentially interfere with cetuximab activity in several different ways, we asked whether activation of ERK1/2 signaling alone was sufficient to phenocopy the effects of *ERBB2* amplification. To this end, we introduced *BRAF* V600E into HCC827 or HN11 cells and evaluated the effects of cetuximab. Both cell lines became resistant to cetuximab (Fig. 2H and fig. S3B), which no longer fully inhibited pERK1/2 (Fig. 2I and fig. S3C). *BRAF* V600E is associated with cetuximab resistance in preclinical models and in CRC patients (*9*). Furthermore, growth factor receptor binding protein 2 (GRB2), a known mediator of ERK1/2 signaling, coprecipitated with ERBB2 in HCC827 CR2 and HN11 cells overexpressing *ERBB2* (Fig. 2J) (*18*). Finally, both GEO and the cetuximab-resistant GEO CR3 cells were equally sensitive to the MEK (mitogen-activated or extracellular signal–regulated protein kinase kinase) inhibitor AZD6244 (fig. S3D). ERBB2 did not inhibit cetuximab binding to EGFR in HCC827 cetuximab-resistant or HN11 ERBB2 cells, nor did it interfere with cetuximab-mediated internalization of EGFR. Collectively, these findings suggest that the principal mechanism by which ERBB2 causes cetuximab resistance is by activating ERK1/2 signaling.

Heregulin mediates resistance to cetuximab in models without evidence of ERBB2 amplification

To determine whether mechanisms other than *ERBB2* amplification could cause cetuximab resistance, we studied a cetuximab-resistant version of A431 cells (Fig. 3A and fig. S5A), which expressed increased levels of pERBB2 and pERBB3 but do not harbor increased total levels of ERBB2 or evidence of an *ERBB2* amplification (Fig. 3B). We hypothesized that these observations may be due to differences in ligands that activate ERBB2/ERBB3 signaling. A431CR cells produced an about 2.5-fold greater concentration of heregulin, measured in an enzyme-linked immunosorbent assay (ELISA), in cell culture medium than did the parental A431 cells (Fig. 3C); this was confirmed by Western blotting (fig. S5B). In the presence of heregulin, ERBB3 preferentially dimerizes with ERBB2 and consequently phosphorylates both ERBB proteins (*19*). Addition of heregulin to A431 cells led to dose-dependent increases in both pERBB2 and pERBB3 (fig. S5C). Furthermore, immunoprecipitation with an anti-ERBB2 antibody showed that in A431CR cells, there was increased association of ERBB2 with ERBB3 compared to the parental A431 cells (Fig. 3D). To examine whether heregulin loss could restore sensitivity to cetuximab in A431CR cells, we depleted heregulin using specific small interfering RNAs (siRNAs) in A431CR cells. Quantitative polymerase chain reaction (qPCR) demonstrated reduced heregulin expression, and immunoblotting revealed lower phosphorylation of both ERBB3 and AKT, a known mediator of ERBB3 signaling (fig. S5D) (*20*). Consistent with these findings, the cells demonstrated greater sensitivity to cetuximab ($P = 0.0007$, t test) (Fig. 3E). We then examined whether exogenous heregulin by itself could lead to resistance in cetuximab-sensitive cell lines. In A431 and the GEO and DiFi CRC cell lines, exogenous heregulin resulted in dose-dependent decreases in cetuximab sensitivity (Fig. 3F and fig. S6A). In the absence of heregulin, cetuximab readily reduced pERK1/2 in all cell lines (Fig. 3G and fig. S6B), whereas in the presence of heregulin, cetuximab had minimal or no effect on ERK1/2 phosphorylation. Heregulin treatment led to ERBB2 and ERBB3 phosphorylation in all three cell lines (Fig. 3G and fig. S6B).

Inhibition of ERBB2 signaling restores cetuximab sensitivity in cells with heregulin-mediated cetuximab resistance

Our studies suggest that ERBB2 activation, and consequently cetuximab resistance, is a result of a heregulin autocrine loop in A431CR cells. To evaluate whether ERBB2 inhibition could represent a potential therapy in such cancers, we evaluated the effects of ERBB2 inhibition on cetuximab sensitivity using several complementary approaches. *ERBB2* depletion with an ERBB2-specific siRNA resulted in increased sensitivity to cetuximab (Fig. 4A). Furthermore, both A431 and A431 cetuximab-resistant cells were equally sensitive to the EGFR/ERBB2 dual kinase inhibitor lapatinib (Fig. 4B). We also treated A431CR cells with pertuzumab, an antibody that disrupts ERBB2/ERBB3 dimerization,

alone and combined with cetuximab (*21*). Neither antibody alone significantly inhibited cell proliferation, whereas the combination of both did (Fig. 4C). Immunoblotting demonstrated that cetuximab was able to down-regulate pERK1/2 in the presence of pertuzumab in A431CR cells, whereas ERK1/2 remained persistently phosphorylated in the absence of pertuzumab (Fig. 4D).

ERBB2 amplification and increased heregulin mediate cetuximab resistance in vivo

Because EGFR-directed antibodies, including cetuximab, have several potential mechanisms of action, not all of which may be apparent in cultured cells, we further evaluated cetuximab resistance in vivo. Both cetuximab and gefitinib effectively inhibited xenografts generated from

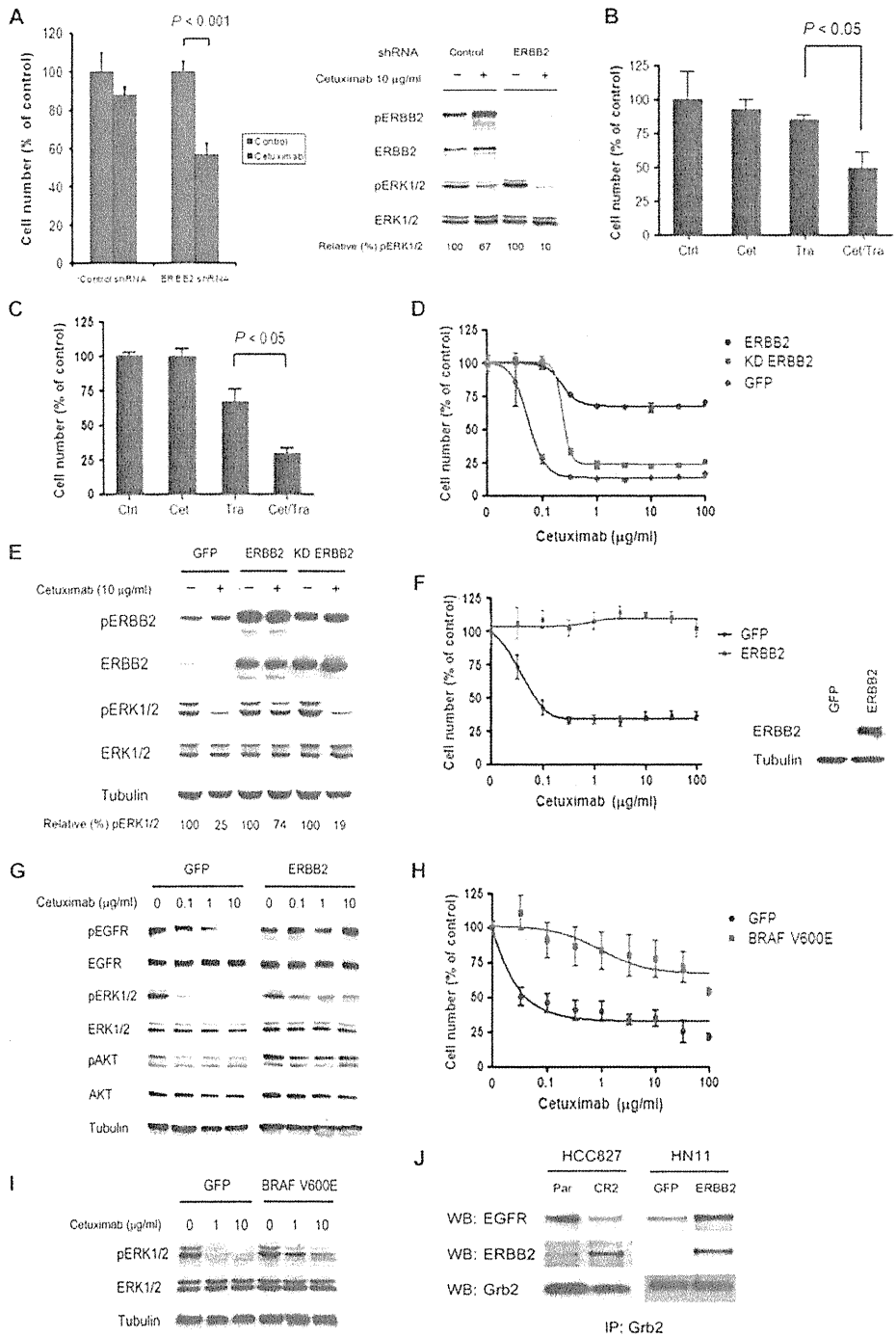

Fig. 2. Inhibition of ERBB2 restores cetuximab sensitivity in cetuximab-resistant cancer cell lines. (**A**) Depletion of *ERBB2* by an ERBB2-specific shRNA restores sensitivity to cetuximab. Control and *ERBB2* shRNA-treated HCC827 CR2 cells were treated with cetuximab (10 μg/ml), and viable cells were measured after 72 hours of treatment and plotted relative to untreated controls. Cell extracts were immunoblotted to detect the indicated proteins. (**B**) HCC827 CR2 cells were treated with cetuximab (Cet) (10 μg/ml) or trastuzumab (Tra) (10 μg/ml) alone or with both agents. Viable cells were measured after 72 hours of treatment and plotted relative to untreated controls (Ctrl). (**C**) GEO CR3 cells were treated with cetuximab (10 μg/ml) or trastuzumab (10 μg/ml) alone or with both agents. Viable cells were measured after 72 hours of treatment and plotted relative to untreated controls. (**D**) HCC827 cells expressing GFP, ERBB2, or kinase-dead (KD) ERBB2 were treated with cetuximab at the indicated concentrations, and viable cells were measured after 72 hours of treatment and plotted (mean ± SD) relative to untreated controls. (**E**) The indicated cell lines from (D) were untreated or treated with cetuximab (10 μg/ml) for 6 hours. Cell extracts were immunoblotted to detect the indicated proteins. (**F**) HN11 cells expressing GFP or ERBB2 were treated with cetuximab at the indicated concentrations, and viable cells were measured after 72 hours of treatment and plotted (mean ± SD) relative to untreated controls. (**G**) HN11 GFP and HN11 ERBB2 cells were treated with the indicated concentrations of cetuximab for 6 hours. Cell extracts were immunoblotted to detect the indicated proteins. (**H**) HN11 cells expressing GFP or BRAFV600E were treated with cetuximab at the indicated concentrations, and viable cells were measured after 72 hours of treatment and plotted (mean ± SD) relative to untreated controls. (**I**) Cells from (H) were treated with the indicated concentrations of cetuximab for 6 hours. Cell extracts were immunoblotted to detect the indicated proteins. (**J**) GRB2 coprecipitates with ERBB2 in HCC827 CR2 and HN11 ERBB2 cells. Cell extracts were immunoprecipitated with an anti-Grb2 antibody. The precipitated proteins were determined by immunoblotting with the indicated antibodies.

GFP-infected HCC827 cells (Fig. 5A), whereas only gefitinib inhibited the growth of HCC827 *ERBB2* xenografts. These tumors were resistant to cetuximab (Fig. 5A), similar to our in vitro observations (fig. S1A). Consistent with its effects on tumor growth, cetuximab treatment led to inhibition of pEGFR and down-regulation of total EGFR in the HCC827 GFP mice (Fig. 5B). In contrast, this was not observed, even after 2 weeks of treatment, in the HCC827 *ERBB2* tumors. Furthermore, ERBB2 coprecipitated with EGFR in the HCC827 ERBB2 tumors, suggesting formation of EGFR/ERBB2 heterodimers in these cetuximab-resistant tumors (Fig. 5B). We also evaluated the effects of cetuximab alone or in combination with pertuzumab in the A431 and A431CR cells (Fig. 5C). Cetuximab alone or in combination with pertuzumab effectively inhibited the growth of A431 xenografts (Fig. 5C). In contrast, only the combination of cetuximab and pertuzumab led to regression of A431CR xenografts (Fig. 5C), consistent with our in vitro findings (Fig. 4C).

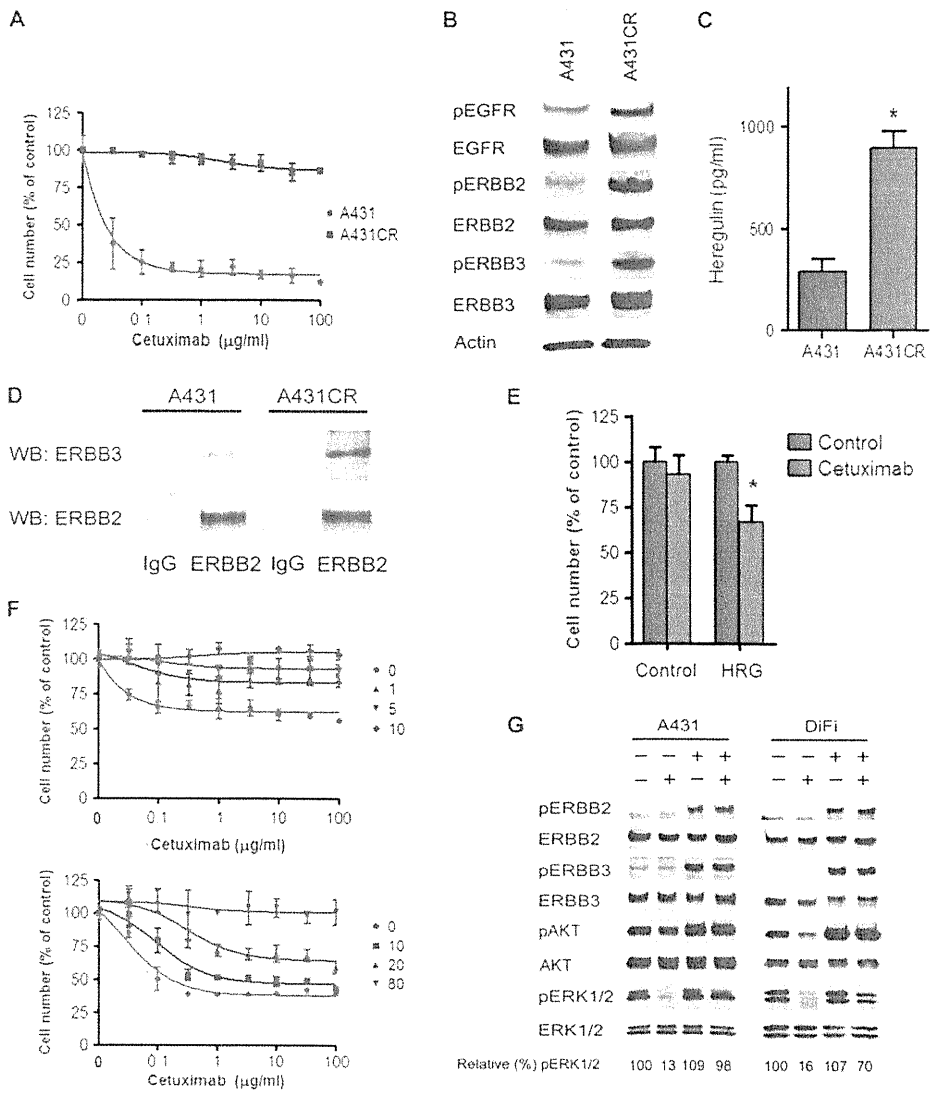

Fig. 3. Heregulin causes resistance to cetuximab. (**A**) Parental and cetuximab-resistant A431 cells were treated with cetuximab at the indicated concentrations, and viable cells were measured after 72 hours of treatment and plotted (mean ± SD) relative to untreated controls. (**B**) A431 cetuximab-resistant cells have increased ERBB2 and ERBB3 phosphorylation. Cell extracts were immunoblotted to detect the indicated proteins. (**C**) Heregulin in cell culture medium was detected by ELISA from A431 and A431CR cells. *P = 0.0021, t test. (**D**) A431 and A431CR cell lysates were immunoprecipitated with anti-ERBB2 antibody. ERBB2 and ERBB3 were detected by immunoblotting. (**E**) Control or heregulin (HRG) siRNAs were transfected into A431CR cells, and cells were treated with cetuximab (100 μg/ml). The percentage of viable cells is shown (mean ± SD) relative to untreated control. *P = 0.0007 compared to control, t test. (**F**) A431 and DiFi cells were treated with cetuximab at the indicated concentrations in the presence of heregulin at the indicated concentrations (ng/ml). Viable cells were measured after 72 hours of treatment and plotted (mean ± SD) relative to untreated controls. (**G**) A431 and DiFi cells were treated with cetuximab (10 μg/ml) alone, heregulin alone (10 ng/ml for A431; 20 ng/ml for DiFi), or the combination. Cells were lysed, and the indicated proteins were detected by immunoblotting.

ERBB2 amplification and increased heregulin are associated with de novo and acquired resistance in cetuximab-treated CRC patients

On the basis of our in vitro and in vivo findings demonstrating a role for both *ERBB2* amplification and heregulin in causing cetuximab resistance, we sought to determine whether these mechanisms also mediate clinical cetuximab resistance. These studies focused on CRC patients because cetuximab is in widespread clinical use in these patients and because our in vitro studies demonstrated that two CRC cell lines, GEO and DiFi, can develop cetuximab resistance through activation of ERBB2 signaling (*1*). We studied *ERBB2* amplification and heregulin as possible mediators of both de novo and acquired cetuximab resistance. Although our preclinical studies focused on mechanisms of acquired cetuximab resistance, we evaluated tumor and blood specimens from cetuximab-treated patients with either de novo or acquired resistance because acquired resistance mechanisms also cause de novo drug resistance as demonstrated for EGFR kinase inhibitors in NSCLC (*22*). We evaluated the clinical impact of de novo *ERBB2* amplification in a cohort of 233 CRC patients (*ERBB2* nonamplified, n = 220; *ERBB2*-amplified, n = 13) who had been treated with cetuximab alone or in combination with chemotherapy (table S1). The median PFS was longer for patients without *ERBB2* amplification (*ERBB2* nonamplified, 149 days; *ERBB2*-amplified, 89 days) (fig. S7). The median OS was significantly longer (*ERBB2* nonamplified, 515 days; *ERBB2*-amplified, 307 days) for patients without evidence of *ERBB2* amplification (P = 0.0013, log-rank test) compared to patients with *ERBB2*-amplified cancers (Fig. 6A). These findings

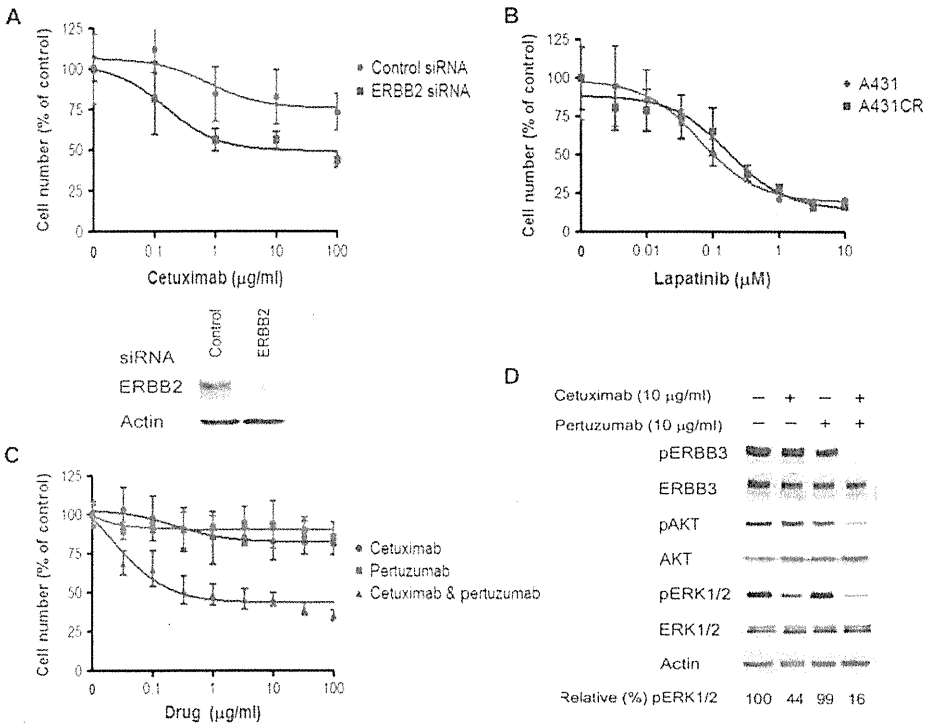

Fig. 4. ERBB2 inhibition restores cetuximab sensitivity in A431 cetuximab-resistant cells. (**A**) Cells transfected with control or ERBB2 siRNA were treated with the indicated concentrations of cetuximab. Viable cells were measured after 72 hours of treatment and plotted (mean ± SD) relative to untreated controls. ERBB2 expression was detected by immunoblotting. (**B**) A431 and A431 cetuximab-resistant cells are equally sensitive to lapatinib. (**C**) A431CR cells were treated with cetuximab alone, pertuzumab alone, or a combination of both drugs at the indicated concentrations, and viable cells were measured (mean ± SD) after 6 days of treatment. (**D**) A431CR cells were exposed to cetuximab alone (10 μg/ml), pertuzumab alone (10 μg/ml), or a combination of both drugs for 6 hours. Cell extracts were immunoblotted to detect the indicated proteins.

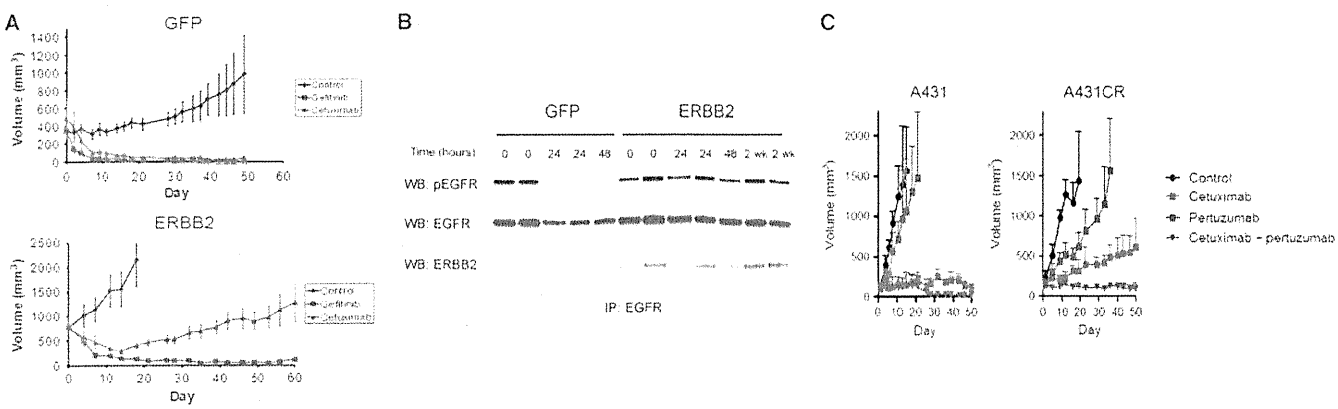

Fig. 5. Both *ERBB2* amplification and heregulin cause cetuximab resistance in vivo. (**A**) Xenografts generated using either HCC827 GFP or ERBB2 cells were treated with vehicle, gefitinib, or cetuximab. Vehicle-treated mice yielded a median tumor size of 2000 mm^3 by 15 days of treatment and were killed. (**B**) Cell extracts from HCC827 GFP or HCC827 ERBB2 tumors treated with cetuximab were immunoprecipitated (IP) with anti-EGFR antibody. Precipitated proteins were determined by immunoblotting with the indicated antibodies. (**C**) Xenografts generated using either A431 or A431 cetuximab-resistant cells were treated with vehicle, cetuximab alone, pertuzumab alone, or a combination of cetuximab and pertuzumab.

were similar when only patients with *KRAS* wild-type tumors were evaluated (Fig. 6A).

To assess a role for *ERBB2* amplification in acquired cetuximab resistance in patient tumors, we evaluated tumor specimens, obtained before and after cetuximab treatment, from two CRC patients who developed clinical cetuximab resistance. In both cases, there were substantially more *ERBB2*-amplified tumor cells in the posttreatment tumors compared to the pretreatment tumors (Fig. 6B and fig. S8A). In a separate cohort of nine patients, we used circulating serum levels of the ERBB2/HER2 ECD as a noninvasive surrogate measure of changes in tumor *ERBB2* after cetuximab treatment (fig. S8B and table S2) (*23*, *24*). In two of nine (22%) patients, both of whom previously had a partial clinical response to cetuximab-based therapy, serum HER2 ECD levels were substantially higher at the time of disease progression than before treatment (fig. S8B).

We also studied the relationship of heregulin to de novo cetuximab resistance in a separate cohort of 70 CRC patients treated with cetuximab-based therapy (table S3). Heregulin levels were evaluated with an ELISA in plasma samples obtained at baseline, before cetuximab exposure. Heregulin concentrations in plasma ranged widely (median, 1622.5 pg/ml; range, 0 to 18,045 pg/ml; Fig. 6C) but were significantly ($P < 0.0001$, t test) lower